KTH Land and Water
Resources Engineering

CO_2 LEAKAGE IN A GEOLOGICAL CARBON SEQUESTRATION SYSTEM: SCENARIO DEVELOPMENT AND ANALYSIS

Farzad Basirat

January 2011

TRITA-LWR Degree Project
ISSN 1651-064X
LWR-EX-11-30

Degree Project in the Water System Technology Master's program

Hydraulic Engineering

Department of Land and Water Resources Engineering

Royal Institute of Technology (KTH)

SE-100 44 STOCKHOLM, Sweden

Reference to this publication should be written as follows: Basirat, F (2011) "CO_2 leakage in a Geological Carbon Sequestration system: Scenario development and analysis" TRITA LWR Degree Project 11:30

SUMMARY IN ENGLISH

Carbon Capture and Sequestration (CCS) is an important method to reduce CO_2 emission into the atmosphere. The sequestration is performed in a geological formation that has the lowest risk for the environment. In this regard, the following three formations are suitable for carbon dioxide storage: a saline aquifer, a depleted oil or gas field and an unmineable coal seam. Among these formations, the saline aquifer is the most used worldwide.

Carbon dioxide leakage is a major concern for Geological Carbon Storage (GCS) performance. The presence of a fracture or faults in the caprock is a potential leakage pathway. To evaluate CO_2 leakage, a tool known as a FEP (features, processes and events) database for CO_2 sequestration is used. The application of the FEP database provides a complete description of the system that is being studied. Moreover, according to system features and processes, several scenarios are defined. The development of these scenarios provides a good knowledge base for a risk analysis of CO_2 sequestration. The scenarios for a geological formation include the presence of formation fluid flow, the salinity of the formation fluid, the reservoir depth and diffusion. In addition, using several modeling approaches to represent fractures (e.g., the equivalent porosity method or the dual porosity or multi-continuum methods) provides additional scenarios for CO_2 leakage.

The modeling and simulations utilized TOUGH2 to model multiphase flow and transport in porous media. TOUGH2 requires a module to model the CO_2-water-salt mixtures. ECO2N is such a module and provides the phase compositions and the component properties of the storage conditions. Results from these simulations suggest that the presence of groundwater has a strong influence on leakage. The reservoir depth also has a significant effect on leakage.

SUMMARY IN SWEDISH

Koldioxidlagring och avskiljning (CCS) är kända och viktiga metoder för minskning av CO2-utsläppen till atmosfären. Koldioxidlagring görs i geologiska formationer som innebär den lägsta risken för utsläpp som kan påverka miljön. Det finns tre huvudsakliga formationer som är lämpliga för koldioxidlagring: saltaquifer, tömda olje-och gasfälter och gammal kolgruvor. Bland dessa formationer är saltakviferer den mest använda för detta syfte i världen. Koldioxidläckage är ett stort problem för geologisk lagring av koldioxid. Förekomsten av små sprickor i bergarten är en av läckagevägarna. För att utvärdera CO2-läckage används ett angreppssätt som kallas FEP (funktioner, processer och händelser). Tillämpningen av olika FEP:er som läggs upp i en databas syftar till att ge en fullständig beskrivning av systemet som skall undersökas. Särskilt definieras flera olika scenarier enligt systemets funktion och dessa processer. Utvecklingen av scenarier ger en god kunskap för riskanalys av CO2-avskiljning. Scenarierna för en geologisk formation omfattar bildandet av vätskeflödet, salthalten av vätskan i formationen, reservoardjupet och diffusionsegenskaper. Dessutom så analyseras olika scenarier för CO2-läckage genom att tillämpning av en rad olika metoder för att modellera spridningen i bergssprickor. Tre kända modeller är porositet-, dubbelporositet- och multi-kontinuum-metoden. I denna studie har modellering genomförts med hjälp av en känd modell som kallas TOUGH2. Den är utvecklad för att modellera flerfasströmning och transport i porösa medier. För att modellera CO2-vatten-salt blandningar behövs ECO2N modulen. ECO2N modulen ger de nödvändiga fassammansättningar och komponenter egenskaper för olika lagringsförhållanden. Resultaten från simuleringarna visar att förekomsten av grundvatten har en stor inverkan på läckage. Reservoardjupet påverkar också läckaget betydligt.

ACKNOWLEDGEMENTS

I would like to express my sincere gratitude to my supervisor, Dr. Lars Marklund, for the invaluable encouragement and support from the early stages of my research to the end. His patient guidance helped me to develop a better understanding of the subject and to become disciplined in my research. I also would like to thank Professor Anders Wörman for giving me the opportunity to be part of his team and to be able to enrich my knowledge under his supervision. I also thank the people in the Division of Geology, in particular Joanna Fernlund for her great help in writing my thesis and Lanru Jing and Vincent Zhihong Zhao for their scientific suggestions. Finally, I would like to thank my family members for their permanent support throughout my life and while conducting my Master's study at KTH.

Stockholm, January 2011

Farzad Basirat

TABLE OF CONTENTS

ABSTRACT

The aim of this project was to study the leakage of CO_2 in a Geological Carbon Sequestration (GCS) system. To define the GCS system, a tool that is known as an FEP database was used. FEPs are the features, processes and events that develop scenarios for the goal of the study. Combinations of these FEPs can produce thousands of scenarios. However, among all of these scenarios, some are more important than others for leakage. The FEPs that were used as scenario developers were the formation of the liquid flow, the salinity of the formation liquid, diffusion as a process for gas bubble transport and the depth of the reservoir layer. In this study, the leakage path is considered as the presence of a fracture in sealed caprock. The fractures can be modeled using various approaches. Here, I represented the influence of fracture modeling by applying the Equivalent Continuum Method (ECM) and the Dual-Porosity and Multi-continuum methods to leakage. This study suggests that considering groundwater in the aquifer would reduce the leakage of CO_2 and that a shallower formation leads to higher leakage. This study can be expanded to future studies by including external FEPs that are related to the FEPs that were used in this study.

Key words: Geological Carbon Sequestration; FEP database; Scenario Development; Saline Aquifer; Leakage; Fracture.

1. INTRODUCTION

A main concern in the geological storage of carbon dioxide is the impact of leakage on the environment and human life. Geological Carbon Storage is a stage in the Carbon Capture and Storage (CCS) method. The aim of keeping CO_2 in geological formations is to reduce the CO_2 concentration in the atmosphere and ultimately control global warming. Carbon dioxide in a reservoir can be retained for a long time using trapping mechanisms. However, the presence of leakage paths (i.e., faults, fractures and leaky wells in geological reservoirs) makes CO_2 storage unsafe.

In this section, the following issues will be explained:

- The necessity of the CCS method for solving the global warming problem
- The current situation of CCS projects around the world
- Geological Carbon Storage and its options
- The safety of geological storage and its risks to the environment
- The mechanisms and processes that lead to CO_2 trapping and leakage within a geological formation

At the end of this section, the objectives and outline of this thesis will be presented.

1.1. Global Warming and CCS

Global warming is a serious threat to environmental systems and human life and is caused by increased concentrations of greenhouse gases in the atmosphere as a result of human activities. Carbon dioxide is the primary greenhouse gas that results from human activities. To mitigate the temperature increase, a reduction in the emission of CO_2 is needed. Various scenarios and strategies have been postulated to reduce CO_2 emissions by the year 2050 (Fig. 1). According to Intergovernmental Panel on Climate Change (IPCC) assessments, CO_2 emissions must be reduced to 50 to 85 percent by 2050 relative to 2000 levels to keep the

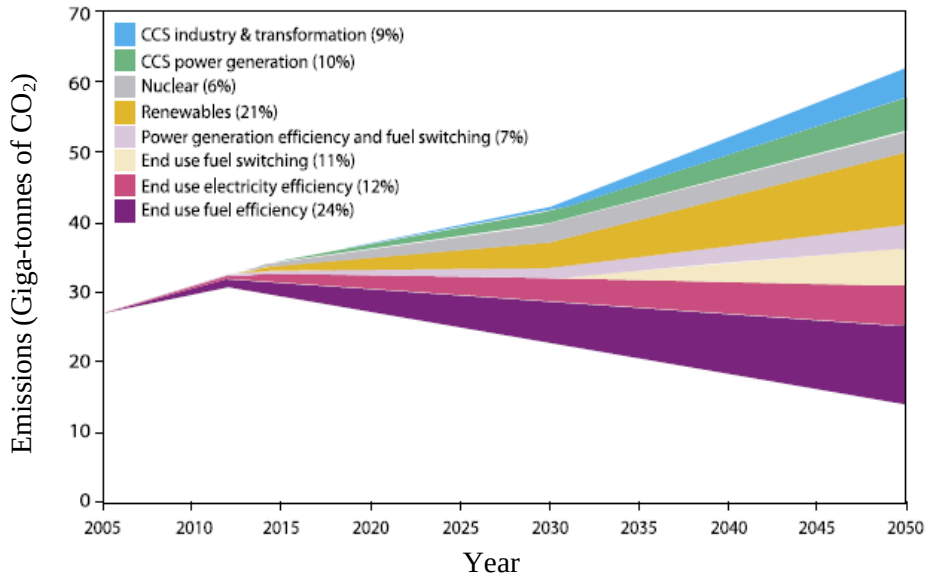

Fig. 1. Estimated rate of CO_2 emission reduction upon implementing the proposed strategies and scenarios by 2050 (IEA, 2008).

global mean temperature rise below 2.0-2.4°C, where severe impacts begin (IPCC, 2007). To achieve the required CO_2 reduction before 2050, it is necessary to reduce CO_2 emissions from fossil fuel power generation and several other vital industries that are not feasible to terminate. Carbon Capture and Storage is the only feasible and effective strategy that can reduce their CO_2 emissions (IEA, 2008).

1.2. Carbon Capture and Storage

Carbon Capture and Storage which is known as CCS, is a technology that reduces CO_2 emissions from point sources such as fossil fuel power plants or plants for manufacturing iron, cement, steel and bulk chemicals (IPCC, 2005). Carbon Capture and Storage consists of the following three steps: capturing the CO_2 at the source point, transporting it to a suitable storage location and finally sequestering the CO_2 using long-term CO_2 storage to reduce the emission of CO_2 into the atmosphere. The storage options are grouped into geological storage, ocean storage and mineral carbonation (IPCC, 2005).

The successful and widespread use of CCS is considered by many key climate change stakeholders to be necessary for achieving deep reductions in CO_2 emissions into the atmosphere. Among a portfolio of reactions such as energy efficiency and renewable energy, CCS is needed to contribute approximately 19 percent of the global CO_2 emission reduction by 2050 (Fig. 1) if global emissions targets are to be achieved (IEA GHG, 2008).

According to an estimate by the IEA, 3,400 industrial-scale CCS projects need to be operational by 2050 to contribute a 19 percent reduction in CO_2 emissions (IEA, 2008). As of 2010, globally there were 77 large-scale integrated CCS projects (LSIPs) planned, of which only 8 are in operation (Table 1). Regarding the number of CCS projects in operation, CCS if far from being used as a widespread, clean and safe method to mitigate global warming.

1.3. Geological Carbon Storage

CO_2 geological sequestration is considered to be the most feasible option for the sequestration of CO_2 (Celia & Nordbotten, 2009; Van der

Zwaan & Smekens, 2009; Yang et al., 2010a). Geological Carbon Storage (GCS) is a process of long-term CO_2 storage within the geosphere. The requirements for successful geological storage are (1) adequate porosity and thickness (storage capacity) and permeability (injection capacity), (2) a satisfactory sealing caprock and (3) a stable geological environment to avoid compromising the integrity of the storage site (Solomon et al., 2008). The three main geologic formations that are used for CO_2 storage (Fig. 2) are oil and gas fields, saline aquifers and coal seams.

Depleted or near-depleted oil and gas reservoirs are the most suitable formations for CO_2 storage for several reasons (Li et al., 2006). First, the oil and gas have been kept there for long time, which provides sufficient storage capacity and a safe caprock. Second, the investigation of oil and gas reservoirs provides sufficient information for CO_2 storage. Third, the available equipment for the extraction of oil and gas can be used. Finally, using CO_2 injection in enhanced gas and oil recovery leads to concurrent CO_2 sequestration (Bachu, 2000). The primary examples of CO_2 storage in depleted oil and gas reservoirs are the Great Plains Synfuel Plant and the Weyburn-Midale Project in the Weyburn reservoir in Saskatchewan, Canada (Wilson & Monea, 2004), and In Salah in Algeria (Riddiford et al., 2003).

The main problem in using depleted oil and gas reservoirs for CO_2 sequestration is their limitation to oil- and gas-producing regions such as Texas and Alberta in North America, the North Sea and the Middle East (Bachu, 2008). Thus, in so many places around the world, other geologic formations such as saline aquifers, coal seams and basalts are considered for the GCS process. Given the widespread global presence of saline aquifers, this would be the next best option following depleted oil and gas reservoirs (Cooper, 2009).

Table 1. The large-scale integrated CCS projects in operation as of 2010 (GCCSI, 2011).

Project name	Location	Capture Type	Transport Type	Storage Type
In Salah	Krechba, Algeria	Gas Processing	14 km pipeline	Geological (Deep Saline Formations)
Sleipner	North Sea, Norway	Gas Processing	Minimal (capture location same as storage location)	Geological (Deep Saline Formations)
Snøhvit	Barents Sea, Norway	Gas Processing	160 km pipeline	Geological (Deep Saline Formations
Great Plains Synfuel Plant and Weyburn-Midale Project	Weyburn, Canada	Pre-Combustion	330 km pipeline	Beneficial Reuse (EOR)
Shute Creek Natural Gas Processing	Southwestern Wyoming, USA	Gas Processing	400km Pipeline	Beneficial Reuse (EOR)
Enid Fertilizer	Oklahoma, USA	Pre-Combustion	192 km pipeline	Beneficial Reuse (EOR)
Val Verde Natural Gas Plants	Sharon Ridge oil field,Texas, USA	Gas Processing	Pipeline (CRC and Val Verde)	Beneficial Reuse (EOR)
Occidental Gas Processing Plant	Pecos County, Texas, USA	Gas Processing	256 km pipeline	Beneficial Reuse (EOR)

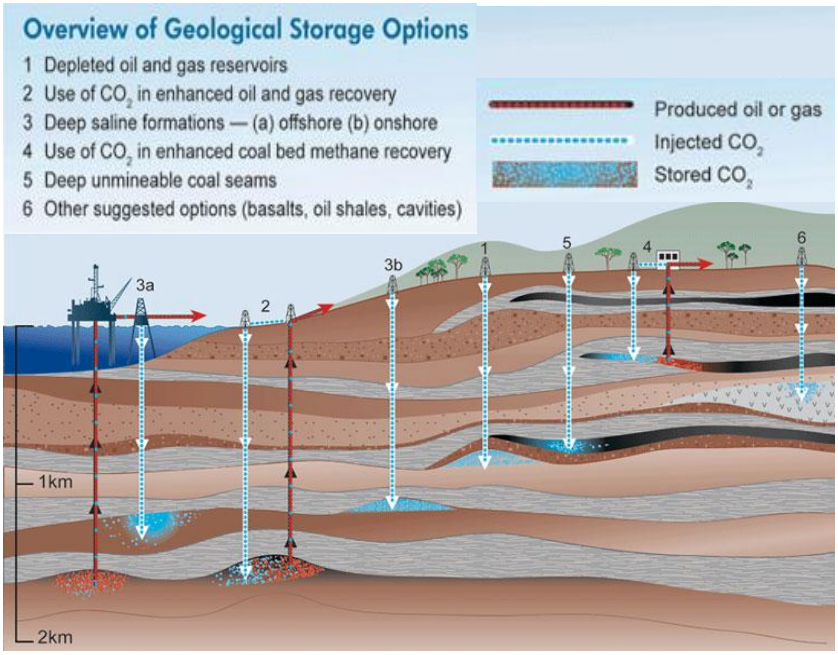

Fig. 2. Geological storage options for CO_2 sequestration (IPCC, 2005).

1.3.1. *Saline Aquifers*

Saline aquifers are present in sedimentary basins throughout the world. Because of their high levels of salinity, these aquifers cannot be used for supplying fresh water (Bachu, 2000) and are commonly used as disposal sites; moreover, in many places, saline aquifers are used to dispose of hazardous chemical waste and liquid radioactive waste (Hesse, 2008; Bachu, 2000).

There are two principal criteria for using saline aquifers for GCS (Bachu, 2003). First, CO_2 must be injected to a depth with appropriate pressure and temperature to maintain the CO_2 in a supercritical state to decrease the storage volume. Second, an impermeable seal overlaying the CO_2 storage is needed to prevent the upward migration of the injected CO_2 toward the surface.

Commercial examples of this type of storage formation include the Sleipner site and the Snøhvit gas field, both of which are in Norway (Table 1). However, the saline aquifers throughout the world cover a range of various environments that differ in location (onshore/offshore), low/high permeability, pressure, temperature and salinity; saline aquifers will be implemented extensively in the future (Oldenburg et al., 2009).

1.3.2. *CO_2 Storage Safety*

As with any industrial activity, the safety of geological carbon dioxide storage must be guaranteed before launching the operation. Safety means that the storage should not be harmful to either human health or the environment. The risks that are associated with CO_2 storage are divided into the following six categories (Damen et al., 2006):

- CO_2 leakage to the surface, which will contaminate the shallow aquifers.
- Contamination of the oil or gas reservoir and the leakage of methane.
- Displacement of brine caused by CO_2 injection in open aquifers, which can contaminate water supplies (Holloway & Savage 1993).

- Micro-Seismicity or even earthquakes of moderate local magnitude (Sminchak et al., 2002).
- Subsidence or uplift of the Earth's surface as a consequence of pressure changes induced by CO_2 injection.
- Contamination of groundwater by heavy metals such as arsenic and lead in shallow aquifers (Zheng et al., 2009).

This project mainly focused on leakage risk due to the potential upward migration of injected CO_2 in a geological reservoir. The potential risk for leakage depends on trapping mechanisms (Bachu et al., 1994; Damen et al., 2006), which are chemical and physical processes that reduce CO_2 buoyancy and mobility (Fig. 3). There is constant balance between trapping mechanisms and leakage mechanisms that determines the CO_2 percentage that remains permanently in storage (Hesse, 2008).

1.3.3. *Leakage Mechanisms*

Carbon dioxide leakage is a major concern for the performance of GCS. Here, leakage is defined as migration across the storage boundary (Oldenburg et al., 2009). Leakage can occur through any of the following paths (Kreft et al., 2007; Gaus, 2010):

- Through openings in the caprock, including fractures, faults or lateral discontinuities.
- Through anthropogenic pathways such as pre-existing wells that were not closed completely or were abandoned.
- Through the pore system in a low-permeable caprock or when CO_2 gas pressure exceeds the capillary pressure in the caprock.

Abandoned wells are the most likely leakage pathways for CO_2 storage due to their high dispersion in many sedimentary basins; for example, there are 350,000 wells in the Alberta basin (Gasda et al., 2004). Leakage

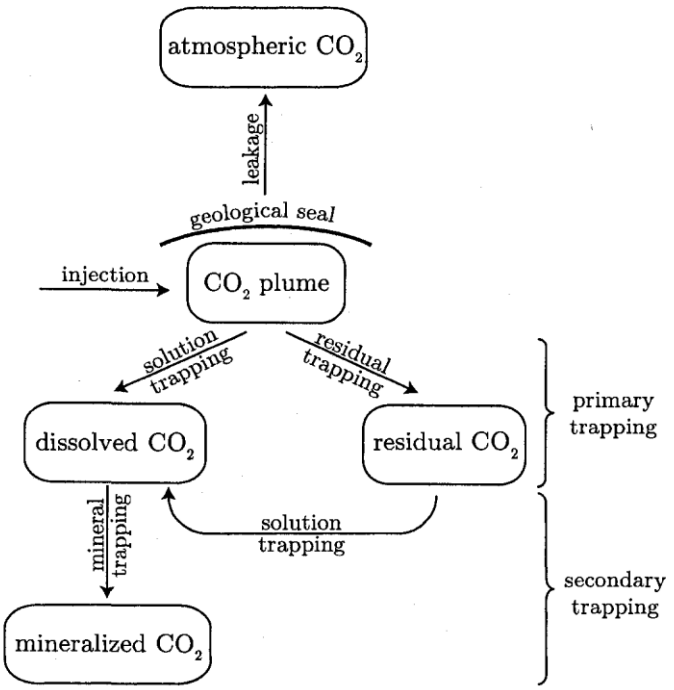

Fig. 3. The different states of CO_2 in geological storage and trapping mechanisms (Hesse, 2008).

through the pore system in low-permeable caprock is a highly improbable scenario and would require the permeability of the caprock and its capillary pressure to be estimated incorrectly (Gaus, 2010).

1.3.4. *Trapping Mechanisms*

Any process that prevents the upward movement of CO_2 and/or an increase in the buoyancy of CO_2 is considered a trapping process (Hesse, 2008). A geological storage site primarily requires a geological seal (caprock) to stop the migration of CO_2 across the storage boundaries (Fig. 3). This process is commonly referred to as structural trapping (or hydrodynamic trapping) (Xu et al., 2004).

There are three trapping mechanisms that are both physically and geochemically dynamic (Fig. 3). The first mechanism is residual trapping, in which a portion of the CO_2 is retained in pore spaces due to capillary forces. Ultimately, the residual trapped CO_2 can dissolve into the formation brine. The second mechanism is dissolution trapping (or solubility trapping), in which CO_2 is dissolved in water. The solubility of CO_2 in brine increases with increasing pressure and decreases with increasing temperature. Because some CO_2 dissolves in the brine, the brine becomes denser and begins to move downward, thereby allowing the CO_2 to become more widely dispersed in the water; over time, the amount of CO_2 dissolved in the water can increase.

The third mechanism is mineral trapping (i.e., the precipitation of dissolved CO_2 upon reaction with rock minerals). Processes related to mineral trapping can occur after a long period of time and will influence the permeability and porosity of the host rock and caprock. In addition, mineral trapping may cause some heavy metals such as lead and arsenic to escape and contaminate the groundwater (Zheng et al., 2009). Mineralization is considered a secondary trapping process because it begins while CO_2 is trapped by dissolution. Both dissolution and residual trapping are therefore considered to be primary trapping mechanisms (Fig. 4).

CO_2 remains in reservoirs in various states, including as plume, residual, dissolved and mineralized CO_2. These states changeover time (Fig. 4).

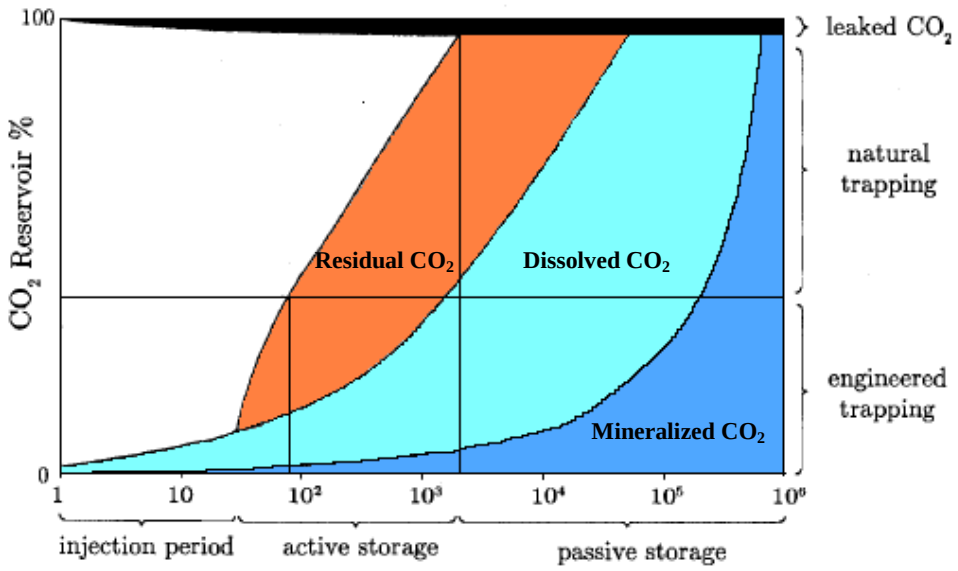

Fig. 4. A schematic diagram of the evolution of the fraction of CO_2 in each state as a function of time (Hesse, 2008).

Dissolution trapping is initiated when CO_2 plumes contact brine and water. Residual trapping is considered to be an important process after the injection process (Kumar et al., 2005). It is possible to improve trapping with engineered trapping such as the injection of brine (Leonenko & Keith, 2008; Hassanzadeh et al., 2009).

1.4. **Project Objective and Outline**

Once a geological storage mechanism is selected for CO_2 sequestration, it is expected to have no leakage path. However, achieving ideal storage without a leakage path is not always possible. Thus, it is expected that a selected reservoir can resist against CO_2 leakage by the presence of leakage paths within the system. The objective of this project is to evaluate the reservoir criteria against leakage. To specify interrelated factors for CO_2 leakage in a reservoir, a System Analysis approach is used. This approach characterizes the features, processes and events that are related to GCS. The System Analysis approach allows for the development of many scenarios that are related to leakage. The characterization of features and processes that lead to more leakage would be helpful in selecting a reservoir for a GCS project.

The outline of this thesis is organized as follows:

Chapter 2: the System Analysis approach that is used for scenario development is explained. A brief description of each scenario is presented in this section.

Chapter 3: the scenarios are described by a list of features, processes and events (FEPs). These FEPs define the reservoir systematically and allow for the recognition of the effective factors of leakage mechanisms.

Chapter 4: the numerical method and tool that are used to evaluate the leakage rate in various scenarios are expressed.

Chapters 5 and 6: the results and discussion, respectively, are presented.

2. LONG-TERM ASSESSMENT OF CO_2 STORAGE

2.1. **Introduction**

As with any industrial activity, the sequestration of carbon dioxide in geological formations may create risks for human health and the environment. Thus, prior to any action, we must ensure the safety of this method. Generally, the feasibility of GCS depends on four factors (Savage et al., 2004). First, the storage volume must be sufficient to provide a significant reduction in CO_2 emission into the atmosphere. Second, the method must be cost-effective. Third, CO_2 storage should be capable of isolating the CO_2 from the atmosphere over prolonged time scales. Finally, the potential impacts on human life and the environment from a GCS project must be within acceptable limits. Therefore, before the implementation of the GCS at any site, a risk assessment that account for all of these factors is necessary.

Risk assessment (RA) is used to select suitable sites from among candidate sites in a process called screening and ranking. In addition, RA is applied in the evaluation and potential certification of specific sites as being both safe and effective (Oldenburg et al., 2009). There are two approaches in the screening and ranking of sites. The first approach was developed by Boweden and Rigg (2004) and uses the RISQUE method, which involves assembling a professional team to expand and rank potential scenarios and events. The second approach, the Screening and Ranking Framework (Oldenburg C.M., 2008), is focused on near-surface risks of CO_2 leakage (Oldenburg et al., 2009). In the evaluation and potential certification of specific sites using a second application of RA,

several approaches are developed, including the System Analysis (Savage et al., 2004), Probabilistic Risk Assessment (PRA) (Rish, 2005), and system modeling approaches (CO_2-PENS) by Stauffer et al. (2009). Among these approaches, the System Analysis Approach is the best known due to its extensive development through nuclear waste disposal risk assessments.

The System Analysis Approach has some advantages that make its application easier. The primary strength of this approach is its systematic side, which provides a high level of confidence in the comprehensiveness of the results (Bouc et al., 2009). This approach is not only useful for initial screening but can also be used as a tool to control other approaches. On the other hand, the System Analysis approach is a time-consuming process due to the need to analyze hundreds of FEPs (features, events and processes) for each site (van Egmond, 2006). In this thesis, the general procedure for the long-term assessment of CO_2 storage using this approach will be described further.

2.2. System Analysis Approach

System analysis consists of the following interconnected elements (Stenhouse et al., 2005):

- A definition of the "system" to be assessed;
- A description of the particular system being studied by an arrangement of the FEPs list;
- A separation of the FEPs that can be regarded as external to the system from the FEPs that define the system itself;
- The identification of an interaction between FEPs;
- A construction of scenarios; and
- A description of how FEP-FEP interactions will be accommodated in subsequent analysis modeling to be undertaken for each scenario.

In this section, following a brief description of the FEPs and FEP databases, each of the system analysis approach elements will be defined for a hypothetical CO_2 storage site.

2.2.1. *FEPs and FEP Database*

FEPs are the factors that are used to define or describe a system and to assess the system's performance. Features include the objects or conditions that may affect the performance of the disposal system. For example, in the case of the geosphere, one feature might be the petrophysical properties such as porosity, permeability, rock grain density, residual saturation and capillary pressure. Events include any natural or human action that influences the system; these usually occur during a short period of time and can include faulting, seismic activity or the intrusion of people into the reservoir (Stenhouse et al., 2005). Processes include the events that operate during all or part of the performance period (Swift et al., 1999). For example, changes in the physical properties of CO_2 with temperature and pressure or the dissolution of CO_2 in situ reservoir fluids are two processes that operate during the performance of a disposal system.

In this study, I used the online FEP database for the geological storage of CO_2 that was developed by Savage et al. (2004) and can be accessed online. The FEPs in this database are relevant to the long-term safety and performance of the sequestration system following the injection of CO_2. The database includes 178 FEPs that are grouped into the following 8 categories (Maul et al., 2005):

1. The Assessment Basis category determines the boundary of the system both in time and place and specifies what is to be assessed and why. The assessment basis of a system contains all of the necessary information that will be used to identify the relevant FEPs. Further assumptions will be explained in the next step of the scenario development.
2. The External Factors category contains FEPs that describe natural and human factors that are outside the system domain but still contribute to the specification of scenarios. It includes three classes of geological factors, climatic factors and future human actions. The external factors are the primary tools that are used for constructing scenarios.
3. The CO_2 Storage category specifies the details of the considered sequestration concept. It has two classes, pre- and post-closure. In the pre-closure class, details of the storage model, the fluids that are injected and the factors for the design, construction, operation and decommissioning phases are described. In the post-closure class, the details of the actions that are performed after the closure of injection are described in detail.
4. The CO_2 Properties, Interactions and Transport category is concerned with the FEPs that are of relevance to the fate of the sequestered fluid. The properties of carbon dioxide can differ widely between conditions at depth and near the surface, and a wide range of physical and chemical reactions can be important.
5. The Geo-sphere category includes the geology, hydrogeology and geochemistry of the storage system. The FEPs in this category describe what is known regarding the natural system prior to the commencement of operations. This category is divided into the following four classes: Geology, Fluids, Geochemistry, and Resources.
6. The Boreholes category is related to the way in which human activity changes the natural system. Boreholes that are used both in the sequestration operations and that have been drilled for other purposes are relevant to the long-term performance of the system.
7. The Near-Surface Environment category describes factors that can be important in the event that sequestered CO_2 returns to the accessible environment. This category is divided into the following three classes: Terrestrial Environment, Marine Environment and Human Behavior.
8. The Impacts category describes any endpoint that could be of interest for an assessment of performance and safety. The impact could be on humans, flora and fauna or on the physical environment.

2.2.2. *Definition of System*

As mentioned above, in the Basis Assessment category, the essential information regarding the system is specified. The basis assessment of the GCS system in this study (Table 2) specifies the site and is comprised of the following components:

- The CO_2 storage reservoir.
- The geosphere, which comprises a number of geological and hydrogeological units above the reservoir.
- The possible pathways for the leakage and migration of CO_2 out of the storage reservoir, for example, fractures and faults.

Table 2. General description of the GCS system according to the Assessment Basis category.

FEP	Description	Audit
1	Purpose of the assessment	To provide a long-term assessment of CO_2 storage in presence of a fractured zone in the caprock.
2	Endpoints of interest	To determine the safety of the storage.
3	Spatial domain of interest	The study domain is CO_2 storage, including the host rock and caprock and aquifers. Near-surface and surface environments are excluded from assessment.
4	Timescales of interest	The timescales may be a thousand years to follow the end of the active period (Fig. 4).
5	Storage assumptions	The rate of CO_2 injection and the total amount injected are model inputs. No other liquid is injected aside from CO_2. Brine is the main geo-fluid (i.e., oil or other hydrocarbons are not included). No major environmental changes are considered either at the surface or at depth.
6	Future human action assumptions	Current human technology is assumed. No societal memory of the storage is assumed.
7	Legal and regulatory framework	Not explicitly considered.
8	Model and data issues	A numerical model is used to evaluate the system.

To define a system with more details, additional features, processes and events are required. Such FEPs are called System FEPs, and these differ from External FEPs, which are not part of the system. External FEPs such as earthquakes, well drilling or new mineral discovery can influence CO_2 storage and migration within the system in which they occur. In such an event, External FEPs (or EFEPs) are known as scenario generators.

Screening and selecting System FEPs is performed according to a system definition that consists of the system domain and the geometry and storage assumptions. Based on this definition, lists of important System FEPs are presented in Table 3. In this table, the FEPs are categorized in different primary groups such as CO_2 properties, CO_2 transport and geosphere, including geology and fluids. Some FEPs were added from the Weyburn CO_2 storage system; however, these FEPs have not been recorded in the database.

2.3. **Scenario Development**

There are always unavoidable uncertainties regarding the future conditions and behavior of CO_2 storage. These uncertainties may arise from different natural processes that act on the system and that range from the occurrence of certain natural phenomena (e.g., seismic events) or from future unpredictable human activities (Stenhouse et al., 2005). Uncertainties regarding the future state of geological storage will be assessed by a calculation of conceptual descriptions of future states that are known as scenarios. From a system analysis approach, a scenario is defined as a hypothetical combination of features, processes and events that is created to illustrate a range of future behavior and states for the disposal system for the purpose of making or evaluating a safety case or for considering the long-term fate of CO_2.

Table 3. List of System FEPs for the CO_2 storage system.

FEP Category	FEP Title
CO_2 Storage	
1	CO_2 quantities, injection rate
CO_2 Properties	
2	Physical properties of CO_2 (density, viscosity, etc.)
3	CO_2 phase behavior (gas, liquid, supercritical liquid)
4	CO_2 solubility and aqueous speciation
CO_2 Transport	
5	Transport of CO_2 (including multiphase flow)
6	Advection of free CO_2
7	Buoyancy-driven flow
8	Capillary pressure
9	Dissolution in formation fluids
10	Dispersion of CO_2
11	Diffusion of CO_2
12	Bubble transport of CO_2
Geosphere Geology	
13	Reservoir geometry
14	Caprock or sealing formation
15	Lithology and mineralogy
16	Heterogeneities
17	Presence and nature of fractures
18	Formation pressure
19	Petrophysical properties
Geosphere Fluids	
20	Fluid properties (composition, geochemistry)
21	Hydraulic pressure
22	Groundwater flow (direction and rate)

When identifying potential scenarios, there is usually one most likely path along which the geological storage system will evolve. This path is known as the Base Scenario and is defined as the expected evolution of the system to be assessed while recognizing that there will be uncertainties associated with this Base Scenario.

2.3.1. *Base Scenario*

- The model domain is the hypothetical storage in a saline aquifer with sufficient space for the injection of CO_2.
- The considered time frame consists of an injection period of 6 years and a hypothetical active period of 1,000 years.
- The caprock may contain natural fractures or discontinuities, but these will all be isolated or sealed so that caprock integrity is not compromised.

- There are a series of aquifer/aquitards above and below the reservoir horizon. These media may contain fractures and/or fissures.
- The base scenario includes a consideration of FEPs that could affect the storage and movement of CO_2. These FEPs include, and are limited to, processes such as hydrodynamics, geochemistry, buoyancy and density-driven flow, the dissolution of CO_2 in water and pressure-temperature changes that occur within the formations.

2.3.2. *Alternate Scenarios*

To define the alternate scenarios, two approaches may be considered. According to the first approach, only scenario-generating FEPs are used as tools. In this regard, the lists of features and processes are assumed to be constant and are not considered to be scenario developers. According to the second approach, a scenario is not limited to a single deterministic future of the system but is a set of similar futures that share common FEPs (Swift et al., 1999). In this method, the number and extent of scenarios depend on the resolution at which FEPs have been defined as such. For example, according to the list of FEPs in Table 3, the scenario resolution is a transport processes. In one scenario, the transport considers advection and diffusion, while in other scenario, the only process is advection. In this project, the second approach is used. A list of feature classes for developing alternate scenarios for this project is defined in Table 4.

Currently, the base scenario and alternate scenarios are generally specified and described. However, to use numerical simulation and modeling for the scenarios, including basis and alternatives, they need to be defined using specific details. Therefore, to define each scenario, it is necessary to know which FEPs are specified for the system. In the next chapter, CO_2 properties, its transport and interaction as well as other important features and processes will be described further. In the end, scenarios with complete details will be prepared.

3. SYSTEM FEPS FOR A CO_2 STORAGE SYSTEM

The features defined for the base scenario are presented in this section. At the end, alternate scenario FEPs will be described. The FEP classes include geology, CO_2 properties, CO_2 transport processes, formation fluid and flow and transport in fractured rock (Table 3). This section is intended to describe each of these FEPs separately; however, because some of these FEPs are closely related, they will be described jointly.

Table 4. List of feature classes for the generation of the alternate scenario.

Alternate Scenario Class	*Description*
Geosphere and fluid formation properties	In this class, the features to be defined for geometry, rock and fluid properties are the tools for scenario generation.
Transport process influence on trapping and leakage	Different transport processes influence leakage, there by generating different scenarios for the system.
Fracture modeling approach	There are different approaches for fracture modeling that may be effective in different trapping mechanisms.
Groundwater flow	The flow of formation fluids may influence CO_2 storage.
Hydraulic pressure (formation pressure)	Formation pressure or hydrostatic pressure is a feature that depends on other FEPs and has a high impact on CO_2 storage.

3.1. **Geology**

Geology includes features that represent the reservoir and surrounding aquifers and rocks prior to the injection of CO_2 (Savage et al., 2004). With the purpose of defining the study system's geology, the features that are represented in the previous section for the geology class (Table 3) are used.

According to the FEP database, the reservoir geometry consists of spatial distribution, depth and the topography of the top surface. The previous chapter, in which the study system was defined, also specified that the system domain is a part of the geosphere, including the host rock (reservoir), caprock and aquifer. Near-surface and surface environments are excluded from the assessment.

The system that is defined herein consists of 3 horizontal layers (Fig. 5). The lowest layer is the reservoir or host rock in which the CO_2 is injected. The middle layer is the caprock, and the upper layer is an aquifer. The system is confined at the top and bottom by impermeable layers, and there is no outflow from the top and bottom boundaries.

Carbon dioxide is injected in a geological storage site in supercritical condition. As a result, the pressure and temperature in the site must be above the critical temperature and pressure of carbon dioxide. Depending on the rate that the temperature increases with depth, the required depth to achieve dense supercritical CO_2 is 800 m or greater (Solomon et al., 2008). The depth of the aquifer layer is 900 m from the surface, and therefore, the bottom of the system is 1,100 m in depth. The depth of the formation influences the hydraulic pressure or the formation pressure. The injection of CO_2 is performed in the middle of the reservoir layer over a 6-year period. The rate of injection is 0.01 kg/sec. The fractured zone is represented by a column inside the caprock layer (Fig. 5).

3.1.1. ***Petrophysical Properties***

The petrophysical properties of the system include features such as permeability, porosity, rock grain density, residual saturation and capillary pressure (Table 5). The data for relative permeability and capillary pressure were obtained from the literature (Pruess et al., 1999). Further information regarding capillary pressure is included in the Appendix I on capillary pressure in CO_2 transport processes. The system domain is assumed to have an isotropic spatial distribution of permeability.

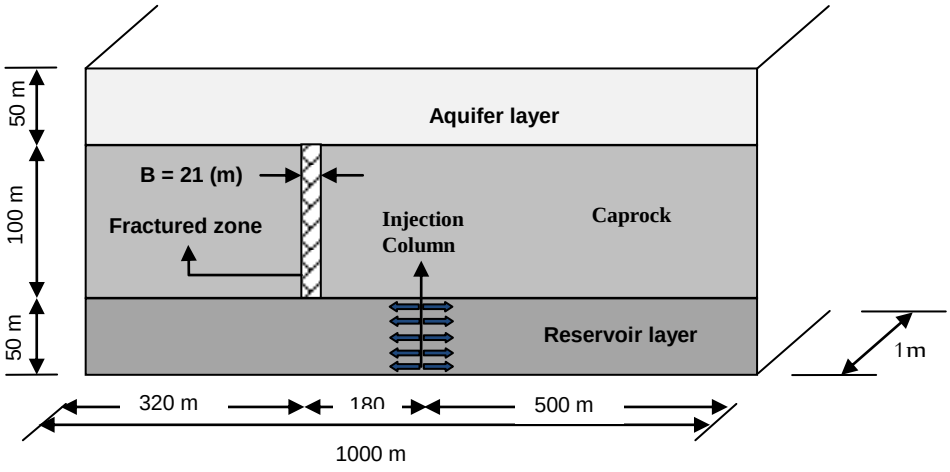

Fig. 5. System geometry and components of CO_2 storage.

Table 5. Petrophysical properties of the CO_2 storage system.

Rock Domain	Rock grain density (kg/m^3)	Porosity	Kx, Horizontal absolute permeability	Kz, Vertical absolute permeability
Reservoir	2600	0.30	4.0E-14	4.0E-14
Caprock	2700	0.08	1.0E-17	1.0E-17
Aquifer	2600	0.325	1.0E-14	1.0E-14
Fracture	2600	0.4	1.0E-12	1.0E-12

Initial values for selected physical parameters

Rock Domain	Lambda	Slr	Sls	Pmax	1/P0
Reservoir	0.457	0.00	1.0	1.0E7	1.6E-4
Caprock	0.457	0.00	1.0	1.0E7	5.1E-6
Aquifer	0.457	0.00	1.0	1.0E7	1.6E-4
Fracture	0.457	0.00	1.0	1.0E7	1.6E-4

Capillary pressure and the parameters for the Van Genuchten (1980) function

Rock Domain	Lambda	Slr	Sls	Sgr
Reservoir	0.457	0.15	1.0	0.05
Caprock	0.457	0.30	1.0	0.05
Aquifer	0.457	0.15	1.0	0.05
Fracture	0.457	0.15	1.0	0.05

Liquid relative permeability and the parameters for the Van Genuchten (1980) function

3.2. CO_2 Properties

The main properties of CO_2 are classified as the physical parameters of CO_2, the phase behavior, CO_2 solubility and aqueous speciation. These properties vary greatly with pressure, temperature and impurities. Due to pressure and temperature variations with changing depth in the geosphere, CO_2 properties need to be modified in the numerical modeling of CO_2 storage.

3.2.1. *Physical Properties of CO_2*

The physical properties of CO_2 (Table 6) include density, viscosity, interfacial tension, thermal conductivity and their dependence on pressure and temperature. The dependence of physical properties on pressure and temperature are important points to consider in finding suitable sites for the geological storage of CO_2.

Carbon dioxide phase behavior depends to a large extent on the variation in pressure and temperature. In standard conditions of temperature and pressure (i.e., temperature of 0°C and an absolute pressure of 100 kPa), CO_2 is in a gas phase. In CO_2 storage, the pressure condition is between 1 and 200 bar and the temperature is expected to range from 10 to 100°C. In a CO_2 sequestration system, CO_2 may be in one of three phases, including the liquid, gas or a supercritical state (Fig. 6).

The supercritical state dominates when the temperature is higher than 31.1°C and the pressure exceeds 73.9 bar (i.e., temperature and pressure are at the critical point) (Span & Wagner, 1998). The thermodynamic properties (i.e., density and viscosity) change when the CO_2 phase changes from liquid or gaseous into a supercritical condition.

Density could suddenly increase as gaseous CO_2 changes to a liquid or supercritical state (Fig. 7a). This sudden jump in the CO_2 pressure-density curves disappears with increasing temperature.

Table 6. Physical properties of CO_2.

Property	Value
Molecular weight	44.01
Critical temperature	31.1°C
Critical pressure	73.9 bar
Critical density	467 kg·m^{-3}
Critical density	467 kg m^{-3}
Gas Phase	
Gas density (1.013 bar at boiling point)	2.814 kg m^{-3}
Gas density (@ STP[a])	1.976 kg m^{-3}
Specific volume (@ STP)	0.506 m^3 kg^{-1}
Cp (@ STP)	0.0364 kJ (mol^{-1} K^{-1})
Cv (@ STP)	0.0278 kJ (mol^{-1} K^{-1})
Cp/Cv (@ STP)	1.308
Viscosity (@ STP)	13.72 µN.s m^{-2} (or µPa.s)
Thermal conductivity (@ STP)	14.65 mW (m K^{-1})
Solubility in water (@ STP)	1.716 vol vol^{-1}
Enthalpy (@ STP)	21.34 kJ mol^{-1}
Entropy (@ STP)	117.2 J mol K^{-1}
Entropy of formation	213.8 J mol K^{-1}
Liquid Phase	
Vapor pressure (at 20 °C)	58.5 bar
Liquid density (at -20 °C and 19.7 bar)	1032 kg m^{-3}
Viscosity (@ STP)	99 µPa.s

[a]Where STP stands for Standard Temperature and Pressure, which is 0°C and 1.013 bar (IPCC, 2005)

For example, in the 20°C curve, there is a sharp density step as the gas phase changes into a liquid phase. However, at 40°C, at which CO_2 is in a supercritical state, after the critical pressure point, there is a continuous density variation after the sharp change in critical pressure. For higher temperatures such as 60°C, there is no distinguishable point to define as the vapor pressure or phase change pressure. In the case of viscosity (Fig. 7.b), the same behavior as for density is observed. The influence of phase behavior is also evident here.

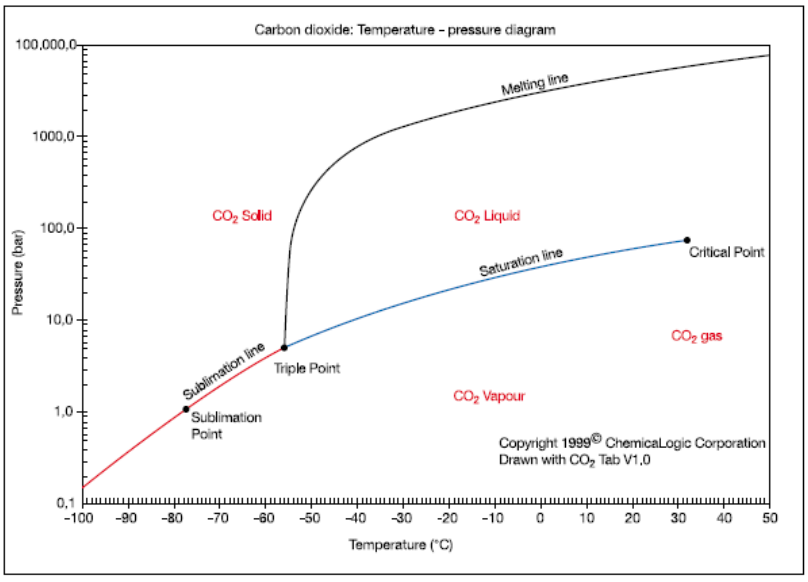

Fig. 6. Phase diagram for CO_2 (Metz et al., 2005).

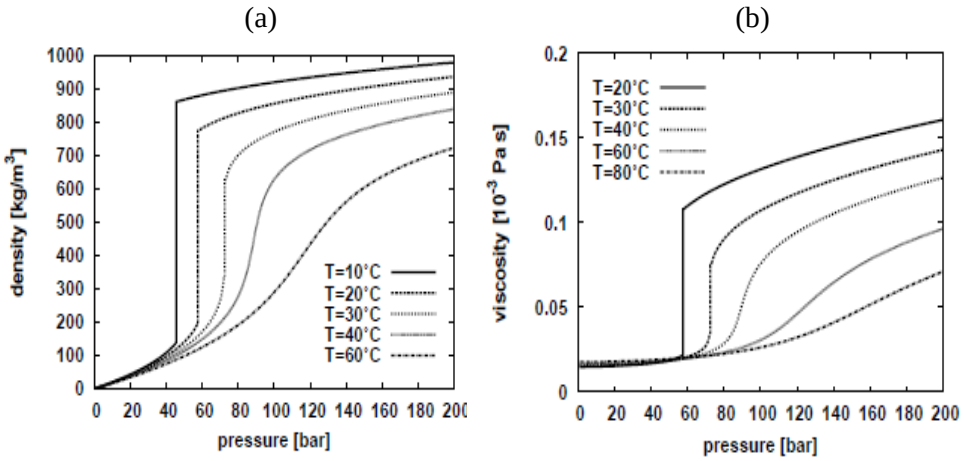

Fig. 7. (a) Density of CO_2 as a function of pressure at various temperatures (b) Viscosity of CO_2 as a function of pressure at various temperatures (Bielinski, 2006).

CO_2 Solubility

The amount of CO_2 that can be dissolved in water is called the CO_2 solubility and is a function of temperature, pressure and salinity and the concentration of any other dissolved species (Fig. 8). CO_2 is present in the aqueous phase as the following: aqueous CO_2, carbonic acid (H_2CO_3), bicarbonate (HCO_3^-) and carbonate (CO_3^{--}). The CO_2 concentration has an impact on the chemical composition of formation fluids, pressure distribution, sorption processes, mineral fluid reactions and the general storage capacity of CO_2 (Savage et al., 2004). CO_2's solubility in water and its separation between the aqueous, gaseous and organic phases controls the effectiveness of diffusive transport and consecutive mineral reactions (Savage et al., 2004).

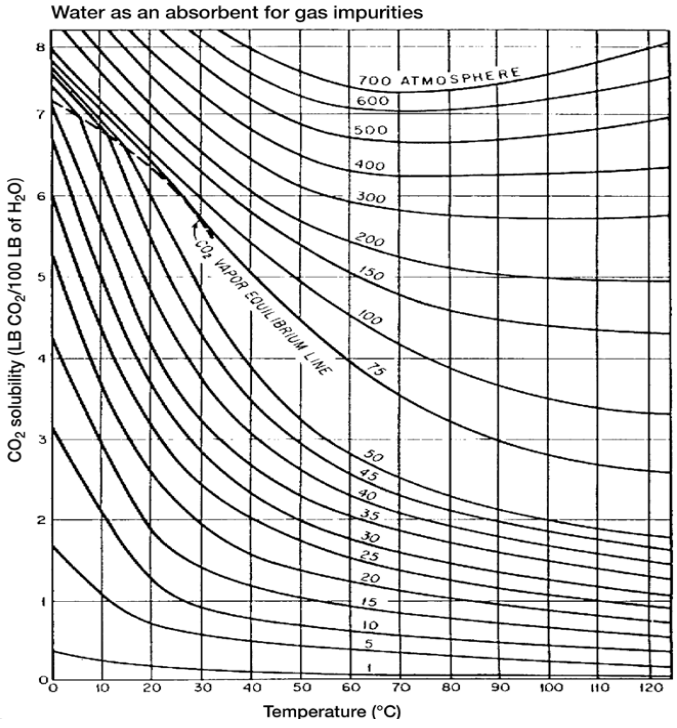

Fig. 8. The solubility of CO_2 in water (Kohl & Nielsen, 1997).

3.3. CO_2 Transport

In this section, the processes and driving forces of CO_2 transport in geological formations are presented. According to the System FEPs (Table 3), eight features are defined for CO_2 transport.

3.3.1. *Advection of Free CO_2*

The advection of CO_2 is caused by a pressure gradient. This pressure gradient may be caused by differences in injection pressure and formation pressure. The rate and direction of advection are a function of the physical properties of the rock such as porosity and permeability (Savage et al., 2004). Dissolved CO_2 can also be transported by advection.

3.3.2. *Buoyancy-Driven Flow*

Buoyancy-driven flow is caused by density differences. In the deep saline aquifer, the free CO_2 that is injected in the supercritical state has less density than brine or water (the formation fluid) and moves upward until it is stopped by the caprock. There is also buoyancy-driven flow of CO_2 that is dissolved in brine. The CO_2-dissolved brine has a higher density than brine without CO_2.

3.3.3. *Capillary Pressure*

Capillary pressure is caused by intermolecular forces that result from cohesion and adhesion and is known as interfacial tension. In other words, the pressure difference caused by interfacial tension across the interface of two immiscible fluids is known as capillary pressure. In a porous media, the capillary pressure (i.e., the interaction between the fluid and the rock matrix) can be modeled as a function of fluid saturation.

The practical application of capillary pressure in CO_2 storage is significant, as there is an interface between two geological layers with different properties. In the case of the reservoir and caprock, there is always a significant difference in their capillary pressures. In the caprock, there is a higher capillary pressure due to its lower permeability relative to the reservoir. Thus, when CO_2 reaches the reservoir and caprock interface, it pools because the entry pressure must increase before it can enter the less permeable layer (Bielinski, 2006).

3.3.4. *Dissolution in Formation Fluid*

Dissolution of CO_2 is considered to be a transport process in the FEP database due to its influence on free-phase CO_2 removal. The dissolution of CO_2 in water creates a new phase in the reservoir. This new phase, which is known as the CO_2 aqueous phase, is water or brine that contains a small percentage of CO_2. The processes of buoyancy-driven flow, diffusion and advection transport dissolve CO_2 and enhance the dissolution rate.

3.3.5. *Diffusion of CO_2*

Diffusion is caused by a gradient of mass and heat concentrations; in other words, diffusion is the process of a component moving from a higher concentration towards a lower concentration. Compared with advection and buoyancy-driven flow, diffusion is extremely slow. Diffusion is an important process for the long-term assessment of a CO_2 plume inside the reservoir.

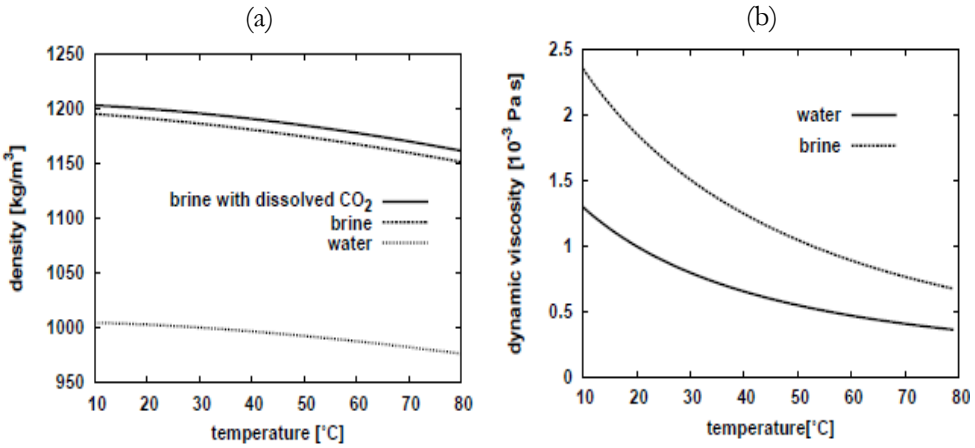

Fig. 9. (a) Water and brine density as a function of temperature. (b) Water and brine viscosity as a function of temperature (at a pressure of 100 bar and salinity of S = 0.25 kg/kg)

3.3.6. *Dispersion of CO_2*

Mechanical dispersion consists of micro-dispersion and macro-dispersion. Micro-dispersion occurs at the pore scale and is caused by the parabolic velocity profile between the grains and velocity variation due to flow paths. On a large scale, macro-dispersion is caused by heterogeneities in the soil matrix. In multiphase systems, there are a few approaches available to quantify dispersion. Because no parameters are available for modeling the geological storage of CO_2, mechanical dispersion is not considered in this project.

3.3.7. *Multiphase Flow of CO_2*

CO_2 sequestration consists of multiphase multi-component flow and transport processes. Multi-component indicates CO_2, water and NaCl in the case of saline aquifers. Under the consideration that there are two components of CO_2 and water present, two different fluid phases would be present in the system (Pruess K., 2005). All sub- and supercritical CO_2 is assumed as a single non-wetting phase, which is referred to as free phase CO_2, and an aqueous phase that is mostly water and may contain some dissolved CO_2.

3.4. Geosphere Fluid

3.4.1. *Brine (Water) Properties*

It is important to understand the physical and chemical properties of brine prior to CO_2 injection. The critical temperature of water is approximately 370°C, and its critical pressure is 220 bar. Thus, unlike CO_2, water cannot change its phase in the system. Therefore, it is in a liquid phase in geological formations.

The density of water is a function of temperature and pressure. Because water density is not as sensitive to pressure as it is to temperature, the influence of temperature on density prevails. As temperature increases, the density of water, brine and CO_2-dissolved brine decreases (Fig. 9.a).

The important parameter in trapping CO_2 is the increase in brine density due to CO_2 dissolution in the brine (Fig. 9.a). Buoyancy-driven forces cause brine that contains dissolved CO_2 to migrate downward and become replaced with brine that does not contain dissolved CO_2. This process enhances the rate of dissolution trapping.

In the case of viscosity, a similar behavior can be observed (Fig. 9.b). Once again, pressure does not produce a significant change. Salinity makes the water more viscous, and temperature has the opposite effect.

3.4.2. *Hydraulic Pressure*

The pressure of formation fluids comes from hydrostatic pressure due to a lack of vertical groundwater flow in the system. Hydrostatic pressure increases with depth at a rate of approximately 10.5 MPa/km for aquifers that are in open contact with surface water (Savage et al., 2004). In this study, the depth of the aquifer starts at 900 m; thus, the pressure at this level is approximately 9.0 MPa, and the bottom of the reservoir is at 1100 m with a pressure of approximately 11.0 MPa. It is presumed that the aquifer and reservoir are in contact with the rest of the subsurface.

3.4.3. *Groundwater Flow (Direction and Rate)*

Groundwater flow is advective and can transport dissolved CO_2. In this matter, groundwater flow can influence the CO_2 plume and CO_2 sequestration. Groundwater flow is caused by a pressure gradient in the aquifer or reservoir.

3.4.4. *CO_2 Interaction*

The only interactions between CO_2 and the media that is considered in this system are mineral dissolution and precipitation. However, it must be mentioned that there are many interactions between CO_2 and a CO_2 sequestration site (including formation fluid displacement, sorption and adsorption of CO_2 and heavy metal release); however, these are excluded from this system.

3.4.5. *Flow Transport in Fractures*

The processes of flow that are defined for the system are also the primary processes for flow and transport in fractures. However, a challenge in fractured rock is generating a model that yields realistic results. There are different approaches for modeling the fracture zone. These principal approaches are as follows (Wu & Qin, 2009):

- The explicit discrete-fracture and matrix model
- The dual-continuum method, including dual- and multi-porosity, dual-permeability, or the more general "multiple interacting continua" (MINC) method
- The effective-continuum method (ECM)

All of these approaches have advantages. Here, however, the dual-continuum approach is used, as it is the primary approach for modeling fluid flow and chemical transport through a fractured reservoir.

Table 6. Features for defining alternate scenarios.

Features Class	Features for defining alternate scenarios
Geosphere geology	Features such as the depth of storage and presence of fractures
CO_2 transport processes	The processes of advection, diffusion, buoyancy driven flow and dissolution
Fluid formation properties	Salinity of the formation fluid (in the base scenario, this is pure water)
Hydrostatic pressure (groundwater flow)	Considering the flow of the formation fluid
Fracture modeling approach	Using ECM, Dual-Continuum and MINC

3.5. Alternate Scenarios

To define alternate scenarios, it is necessary to change one or more of the features that were used in the Base scenario. Using all of the features provides several hundred scenarios.

Due to these scenarios, some FEPs are considered to be more interesting to study than others (Table 6). Based on each of the considered FEPs, alternate scenarios are formed (Table 7). For example, in the first alternate scenario (A-1), it is assumed that no fracture is present in the caprock.

This scenario provides the difference in the storage of CO_2 in both the presence and absence of fractures in the caprock.

4. NUMERICAL MODELING

This section explains the tool and method that were used for defining the system components in Section 3. In addition, the general setups for the simulation in all of the scenarios are described.

4.1. TOUGH2

The tool that was used in this project is a code known as TOUGH2 (transport of unsaturated groundwater and heat). TOUGH2 is a numerical simulation program that was developed for non-isothermal flows of multiphase, multi-component fluid mixtures in porous and fractured media (Pruess, 1991; Pruess et al., 1999). The primary purpose for developing TOUGH2 was for use geothermal reservoir engineering, nuclear waste isolation studies, environmental assessment and remediation and flow and transport in variably saturated media and aquifers (Pruess et al., 1999).

Before using TOUGH2 as a computational simulation tool, it is necessary to verify that TOUGH2 can solve the problem that is defined herein. In this respect, the physical and mathematical models of TOUGH2 are briefly introduced here. In addition to the physical processes, a brief description of the numerical method is also presented.

4.1.1. *Physical Processes*

The physical processes that are considered in TOUGH2 consist of fluid flow in both the liquid and gas phases that occur under pressure, viscous, and gravity forces; relative permeability and capillary flow; heat flow by conduction and convection; and diffusive mass transport in all phases (Pruess et al., 1999). All thermo-physical parameters are calculated as a function of temperature and include fluid (gas and liquid) density and viscosity. The dissolution of gas in water is represented by Henry's law.

Table 7. Alternate scenarios.

Alternate scenario name	Description
A-1	No fracture zone is present in the caprock
A-2	Diffusion is not considered as a transport process
A-3	System depth is changed and is located at a depth of 600 m below the ground surface
A-4	Flow of water in the reservoir layer
A-5	Flow of water in the aquifer layer
A-6	Formation fluid has a salinity of 10 ppm
A-7	Using ECM instead of DCM
A-8	Using MINC instead of DCM

4.1.2. *Governing Equation*

The basic mass and energy balance equation that is used in TOUGH2 in the general form is written as follows:

$$\frac{d}{dt}\int_{V_n} M^K \, dV_n = \int_{\Gamma_n} \mathbf{F}^K \cdot \mathbf{n} d\Gamma_n + \int_{V_n} q^K dV_n \qquad \text{Eq. 1}$$

This equation consists of the following three primary terms: a mass accumulation term, a mass flux term and sink and a source term. The integration is performed over an arbitrary sub-domain of V_n of the flow system under study that is restricted by closed surface Γ_n.

The mass accumulation term, M, represents mass and energy per volume. The superscript K = 1 … NK represents the mass components (water, CO_2 and salt). The general format of the mass accumulation term is as follows:

$$M^K = \emptyset \sum_{\beta} S_\beta \rho_\beta X_\beta^K \qquad \text{Eq. 2}$$

The total mass of component K is obtained by summing the fluid phase β (liquid, gas), and Φ is porosity, S_β is the saturation of phase β, ϱ_β is the density of phase β, and X_β^K is the mass fraction of the component K that is present in the phase β. For the heat component, heat replaces mass. Because in this project all of the scenarios are simulated for isothermal conditions, there is no need to discuss the formulation of heat mass accumulation and heat flux equations. The second term is the mass flux term and contains the sums over phases as follows:

$$\mathbf{F}^{(K)} = \sum_{\beta=l,g} \mathbf{F}_\beta^{(K)} \qquad \text{Eq. 3}$$

In which the flux in each phase is calculated by the following multiphase version of Darcy's law:

$$\mathbf{F}_\beta = \rho_\beta \mathbf{u}_\beta = -k \frac{k_{r\beta}\rho_\beta}{\mu_\beta}\left(\nabla P_\beta - \rho_\beta \mathbf{g}\right) \qquad \text{Eq. 4}$$

In this equation, $\mathbf{u}_\beta$ is the Darcy velocity (flux volume) in phase β, k is absolute permeability, $k_{r\beta}$ is the relative permeability of phase β, μ_β is viscosity of phase β, P_β is the pressure in phase β, and g is the gravitational acceleration. The pressure in phase β is the sum of pressure P of the reference phase and capillary pressure ($P_{C\beta}$). In addition to the advective flux above, there is diffusive transport (Appendix I).

The last term in Eq.1 is the sink and source term, and q_K denotes the sinks and sources. Other equations and formulae that are included in TOUGH2 are presented in Appendix I.

4.1.3. *Fluid Property Module for CO_2 Sequestration (ECO_2N)*

For CO_2 sequestration modeling in TOUGH2, a fluid property module has been developed, which is known as ECO_2N. ECO_2N can be used to model the geological storage of CO_2 in saline aquifers (Pruess &

Spycher, 2007) and includes a complete explanation of the thermodynamics and thermo-physical properties of H_2O–NaCl–CO_2 mixtures in the temperature, pressure and salinity conditions of interest (10°C < T < 110°C; P < 600 bar; salinity up to full halite saturation) (Pruess & Spycher, 2007).

In the ECO_2N module, the thermo-physical properties of the CO_2 gas phase and liquid phase are defined; however, for the treatment of flow, no distinction is defined between these properties. In addition, no phase change between the gaseous and liquid phases is considered. In this module, carbon dioxide in both the sub- and supercritical conditions is considered as a single non-wetting phase and is referred to as "gas".

There are four primary variables defined in the ECO_2N module to reach the conditions for the CO_2-brine system. A summary of the components and phases that are modeled by ECO_2N and the primary variables for the system are presented in Table 8. The second primary variable is Xsm, which is the salt mass fraction in the water and salt system and is denoted as Xs when there is no solid salt present in the system. When there is solid salt in the system, Xs is determined by the equilibrium solubility of NaCl, which is a function of temperature (Pruess K., 2005). Here, Xsm = Ss + 10, where Ss is defined in analogy to fluid saturations and denotes the fraction of void space that is occupied by solid salt. The physical range of both Xs and Ss is (0, 1), and 10 is used only for the separation between the presence and absence of solid salt in the system.

X3 is the third primary variable and denotes the CO_2 mass fraction (X2) under single-phase conditions (i.e., only aqueous or only gas). Two-phase (aqueous and gas) conditions are defined as gas saturation plus ten (Sg +10). Here, "10" is added to differentiate two-phase conditions from the single phase condition.

In ECO_2N, several correlations have been developed (Spycher & Pruess, 2007) to define the prediction of the equilibrium composition of the liquid (aqueous) and gas (CO_2-rich) phases as functions of temperature, pressure, and salinity that are valid for their ranges in CO_2 sequestration systems.

Table 8. Summary of the variables in the ECO_2N module (From Pruess K., 2005).

Components:	# 1: water # 2: NaCl # 3: CO_2
Parameter choices:	(NK, NEQ, NPH, NB)
(3, 4, 3, 6)	water, NaCl, CO_2, non-isothermal (default)
(3, 3, 3, 6)	water, NaCl, CO_2, isothermal
• molecular diffusion can be modeled by setting NB = 8	
Primary Variables:	
single-fluid phase (only aqueous or only gas) # (P, Xsm, X3, T)	
P - pressure Xsm - salt mass fraction Xs in two-component water-salt system, or solid saturation Ss+10 X3 - CO_2 mass fraction in the aqueous phase, or in the gas phase, in the three-component system water-salt-CO_2 T – temperature T - temperature	
two-fluid phases (aqueous and gas)# (P, Xsm, Sg+10, T)	
P - pressure Xsm - salt mass fraction Xs in two-component water-salt system, or solid saturation Ss+10 Sg - gas phase saturation T - temperature	

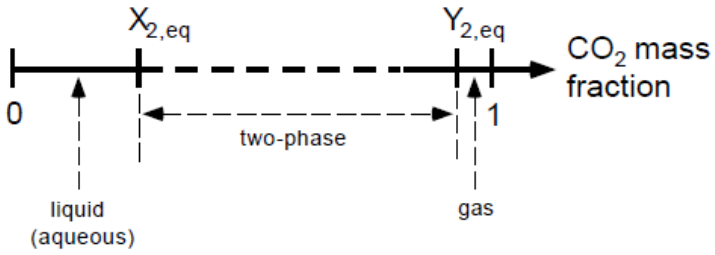

Fig. 10. CO_2 phase partitioning in the system H2O - NaCl - CO_2.

The correlation between CO_2 mass fraction X3 and the phase composition of the fluid mixture is as follows (Fig. 10):

- X3 < X2eq corresponds to single-phase liquid conditions;
- X3 > Y2eq corresponds to single-phase gas;
- X2eq ≤ X3 ≤ Y2eq corresponds to two-phase conditions.

in which $X_{2,eq}$ corresponds to a dissolved CO_2 mass fraction in the aqueous phase that is smaller than 0.01 and $Y_{2,eq}$ is the gas phase CO_2 mass fraction in a gas phase that is larger than 0.99. Additional technical information and applications procedures of TOUGH2 and ECO_2N are available in the ECO_2N manual by Pruess (2005).

4.2. Numerical Approach

The numerical approach that is used in TOUGH2 for space discretization is the integral finite difference method (IFDM; Edwards, 1972; Narasimhan & Witherspoon, 1976). The advantages of IFDM include the lack of a need of a reference to a global system of coordinates and that it is applicable to both regular and irregular discretizations in all dimensions. In addition, IFDM can be used in the multi-porosity method for fractured media. For time discretization, a full implicit first-order backward finite difference is used.

Discretization results in a set of tightly coupled nonlinear algebraic equations with the time-dependent primary thermodynamic variables of all of the grid blocks represented as unknowns. These equations are solved simultaneously using the Newton-Raphson iteration method. Time steps can be automatically stepped (increased or reduced) during a simulation run, depending on the convergence rate of the iteration process. Different methods are used to solve the linear equations at each iteration step, including preconditioned conjugate gradient solvers as well as sparse direct matrix methods (Pruess et al., 1999).

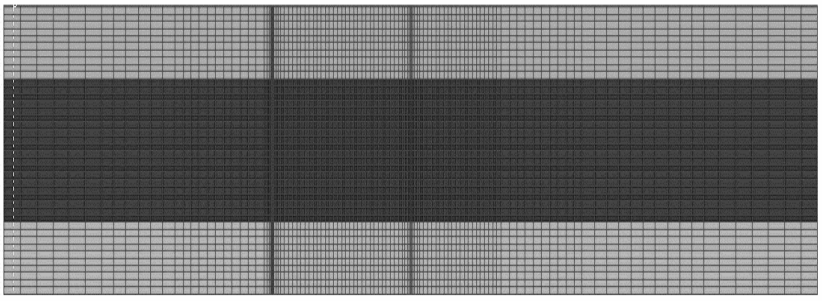

Fig. 11. The mesh generated for simulation.

4.2.1. *Model Simulation*

General Setup

The geometry of the system (Fig. 5) is kept constant for all simulations and alternate scenarios. The injection well with a constant flow rate is situated in the middle of the reservoir. CO_2 is injected through entire height of the reservoir layer and is called the injection column.

The model axes are oriented with the aquifer geometry. The Z-axis is perpendicular to the system layering, and the X-axis is parallel to it. For the simulations, the following assumptions are considered:

- The porous medium is rigid and does not participate in any reactions.
- Friction between the water phase and the CO_2 phase is not taken into account.

Description of the Used Mesh

The mesh that is generated for the system is shown in Figure 11. Fine meshes that are close to the injection column and the fracture zone were used. The total amount of elements in the system is 4,880. The element heights are constant at a value of 5 m; thus, the total number of cells in the Z-direction is 40. In the X-direction, the elements close to the boundaries are wider, where as the width of the elements closer to the injection cells is smaller. The total number of elements in the X-direction is 122. For generating the elements, the tool Mesh Maker in TOUGH2 was used.

Initial Values and Boundary Conditions

The initial values and boundary conditions for the simulation of the base model are listed in Table 9. Other parameters that are used are described in Section 3 (FEPs). The initial values and boundary values for the alternate scenarios are described in Appendix II.

Table 9. Initial and boundaries condition of the Base scenario.

Initial Condition: Only water phase					
Variable	**Value**	**Unit**	**Comment**		
CO_2 mass fraction in brine (X3)	00.0	----	CO_2 in the aqueous phase can be present in the geosphere in very low value, so it can be assumed initially to be zero		
Salt mass fraction (Xcm)	00.0	ppm	No salt in the water		
Temperature (T)	39.0	˚C	Temperature is assumed to be constant with depth		
Boundary conditions:					
boundary	**type**	**variable**	**value**	**unit**	**Comment**
Top & Bottom	Neumann	Qw	00.0	Kg/(m^2.sec)	no-flow (Water)
	Neumann	Q_{CO2}	00.0	Kg/(m^2.sec)	no-flow (CO_2)
Left & Right	Dirichlet	X3	00.0	----	
	Dirichlet	Xcm	00.0	ppm	
	Dirichlet	T	39.0	˚C	
	Dirichlet	P	90.0E5+ 9.80*z(m)	Pa	

5. RESULTS

This section describes the simulation results for each scenario as explained in Section 3. The results consist of the evolution of the CO_2 plume and dissolved CO_2 in the system domain, the CO_2 mass quantity in each layer and finally the CO_2 leakage rates from the fracture zone outlet. A comparison between scenarios was used to visualize the influence of the various study features and processes on the CO_2 sequestration system.

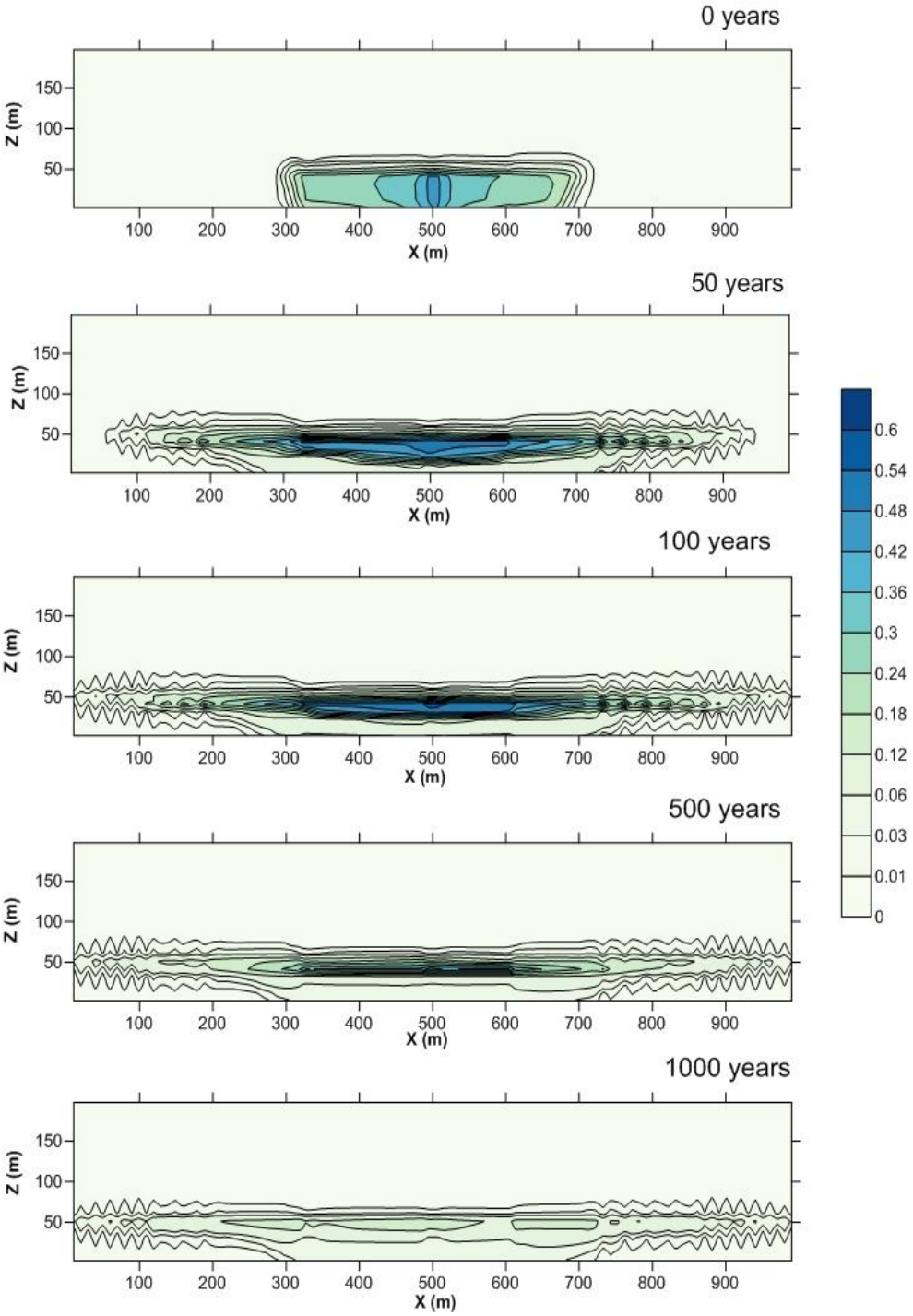

Fig. 12. Supercritical CO_2 gas phase (SG) migration in the system without a fractured zone simulated from the end of the injection until 1,000 years later.

5.1. **No Fractured Zone (Scenario A-1)**

This scenario represents CO_2 behavior in the desirable and favorable situation for a CO_2 sequestration system. The presence of a sealed caprock with low permeability in this scenario produces results that are distinguishable from other scenarios. There is no CO_2 leakage into the aquifer layer for 1,000 years following the injection time (Fig. 12). After the injection of CO_2 in the supercritical condition, free CO_2 moves into the left and right sides of the injection column.

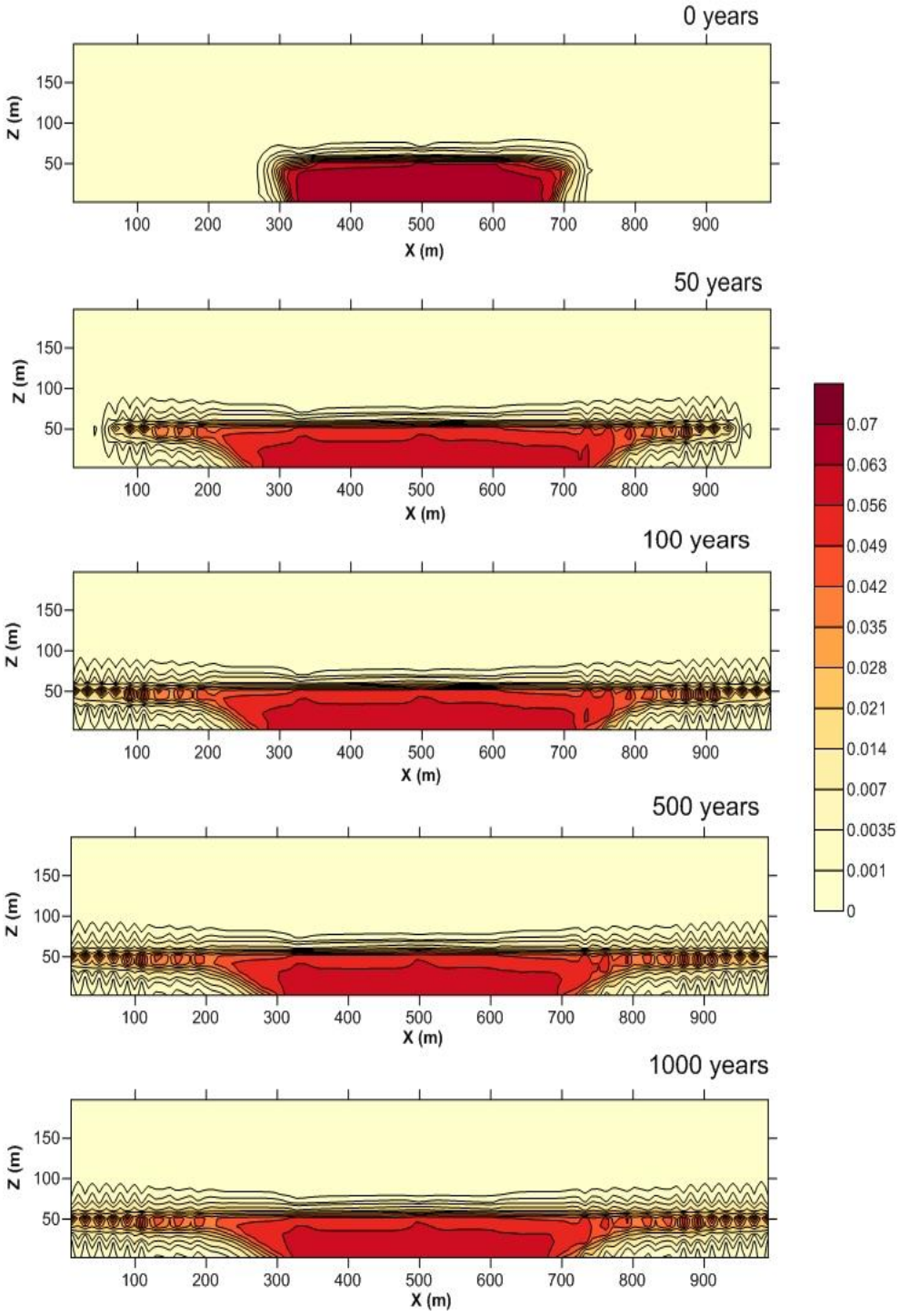

Fig. 13. Mass fraction of CO_2 in the water (XCO_2L) for the CO_2 sequestration system without a fracture zone simulated from the end of the injection until 1,000 years later.

At the end of the injection, CO_2 moves upwards and expands into the bottom of the caprock. As time passes, the single phase of CO_2 decreases and the gas saturation in the entire reservoir is reduced correspondingly. In addition, a low amount of CO_2 moves into the caprock in the free phase (Fig. 12).

As time passes, the aqueous phase contains dissolved CO_2 (Fig. 13) that is transported into the entire reservoir. Here, the growth of the aqueous phase containing more dissolved CO_2 has a shape that is similar to free-phase CO_2. Unlike free-phase CO_2, the aqueous phase that contains a higher fraction of dissolved CO_2 moves downwards.

The curve of the total amount of CO_2 in the reservoir has three stages (Fig. 14). The first stage represents the injection period, in which the total CO_2 increases constantly. In the second stage, the amount of CO_2 remains moderately constant within the reservoir. Approximately 100 years after the injection, the total CO_2 amount is reduced in the reservoir. The behavior of free CO_2 in the reservoir is similar to the total CO_2. However, for dissolved CO_2, there are two stages, the injection period and the period following the injection, which have lower rates than the injection period (Fig. 14.b).

Compared with the reservoir, the caprock contains a lower amount of CO_2; however, the CO_2 phase behaves completely differently in the reservoir (Fig. 14.a). In both the caprock and reservoir, total CO_2 has three stages. However, in contrast to the reservoir, in the caprock there is no reduction after 100 years. After 100 years, there are changes only in the increase rate, and the CO_2 slope declines. Here, most of the CO_2 is in a dissolved phase. In the injection period, the amount of free CO_2 is approximately zero, but as time passes, the amount of free-phase CO_2 also increases. However, after 100 years, this increase stops; after approximately 500 years, the amount of free CO_2 is reduced.

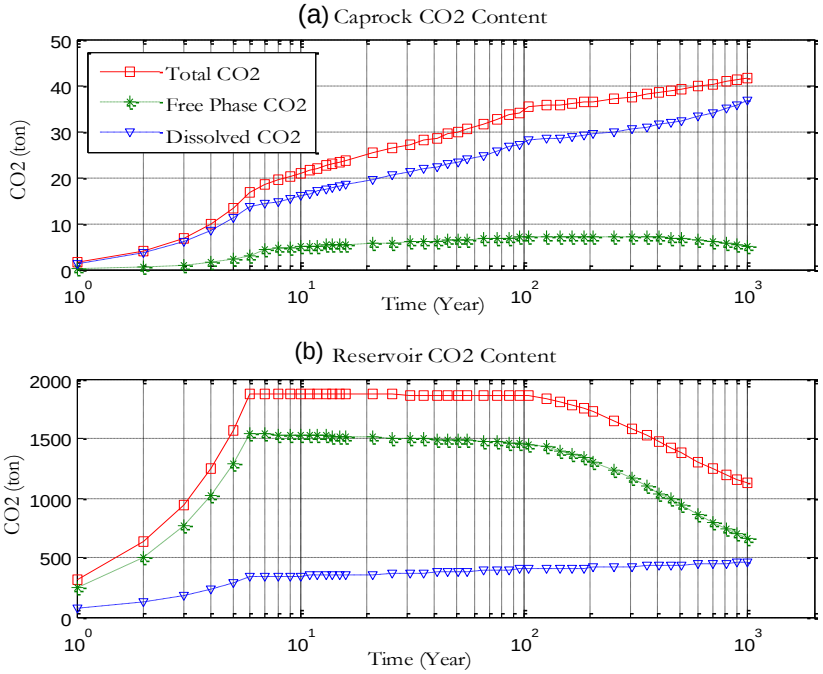

Fig. 14. CO_2 phase mass (free and dissolved) in a system without a fracture zone in the a) Caprock or b) Reservoir.

5.2. **Fractured Caprock (Base Scenario)**

As it was defined above, this scenario includes a single fracture at 170 m from the injection column. In this scenario, CO_2 in the free phase leaks into the aquifer layer during the injection period (Fig. 15). The CO_2 plume in this scenario is asymmetrical, and the free CO_2 does not reach the left boundary of the system in the reservoir layer. The leakage of CO_2 reduces as time passes. Dissolved CO_2 in the aqueous phase has a shape that is similar to the gas phase (Fig. 16).

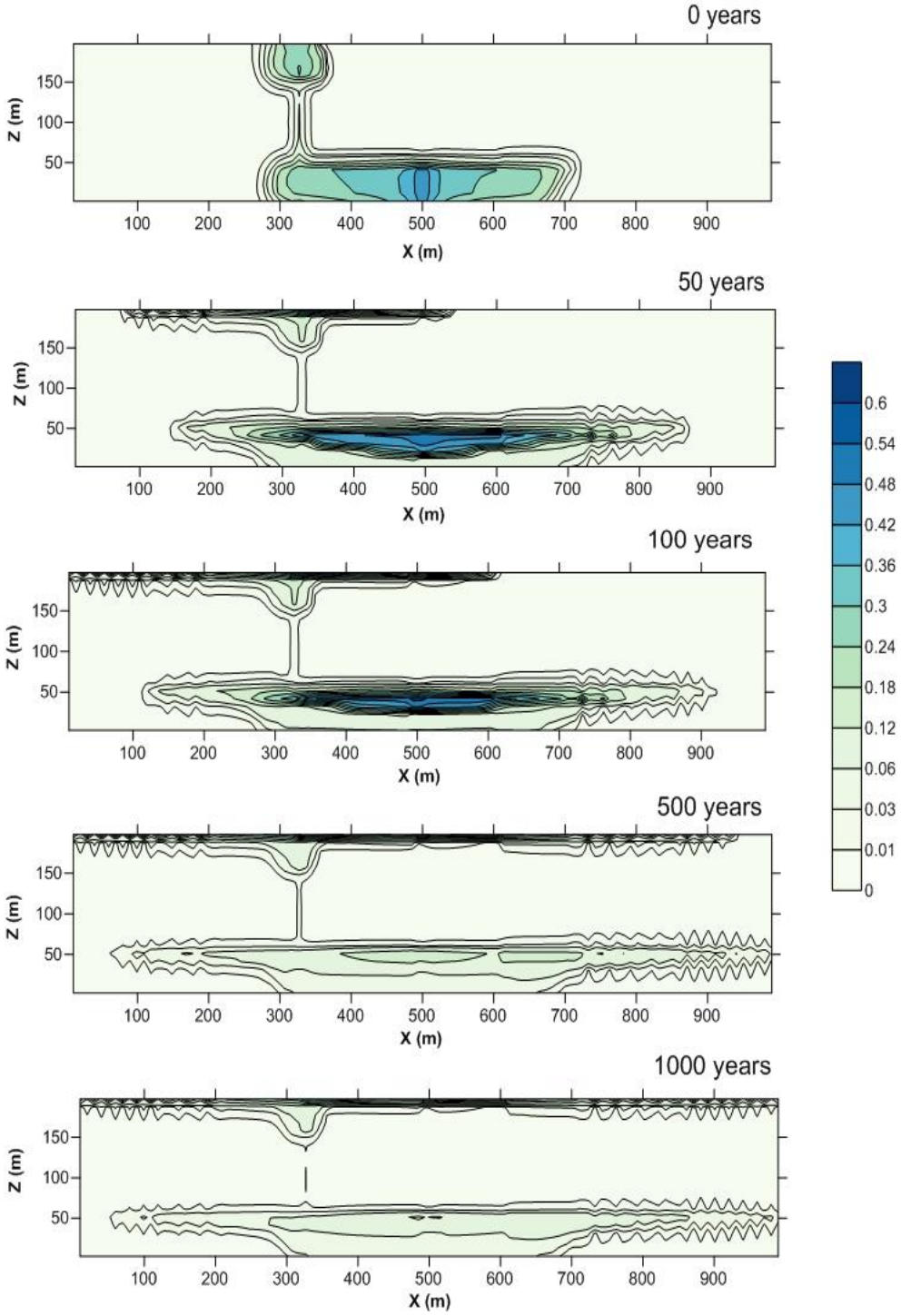

Fig. 15. Supercritical CO_2 gas phase (SG) migration in the system with a fractured zone (Base Scenario) simulated from the end of the injection period until 1,000 years later.

Compared with the non-fracture case, the mass fraction of CO_2 at the end of the injection period is transported a further distance. In the non-fracture case, the dissolved CO_2 moves 200 m from the injection point and has a constant value within the entire area (Fig. 16). The total amount of CO_2, in both the dissolved and single phases varies with time in the different system layers (Fig. 17).

In the reservoir, three stages for free-phase CO_2 can be distinguished. The first stage is during the injection period, and the second stage occurs 100 years after the injection; the third stage is from 100 to 1,000 years, in which free-phase CO_2 declines more than it did in the second stage.

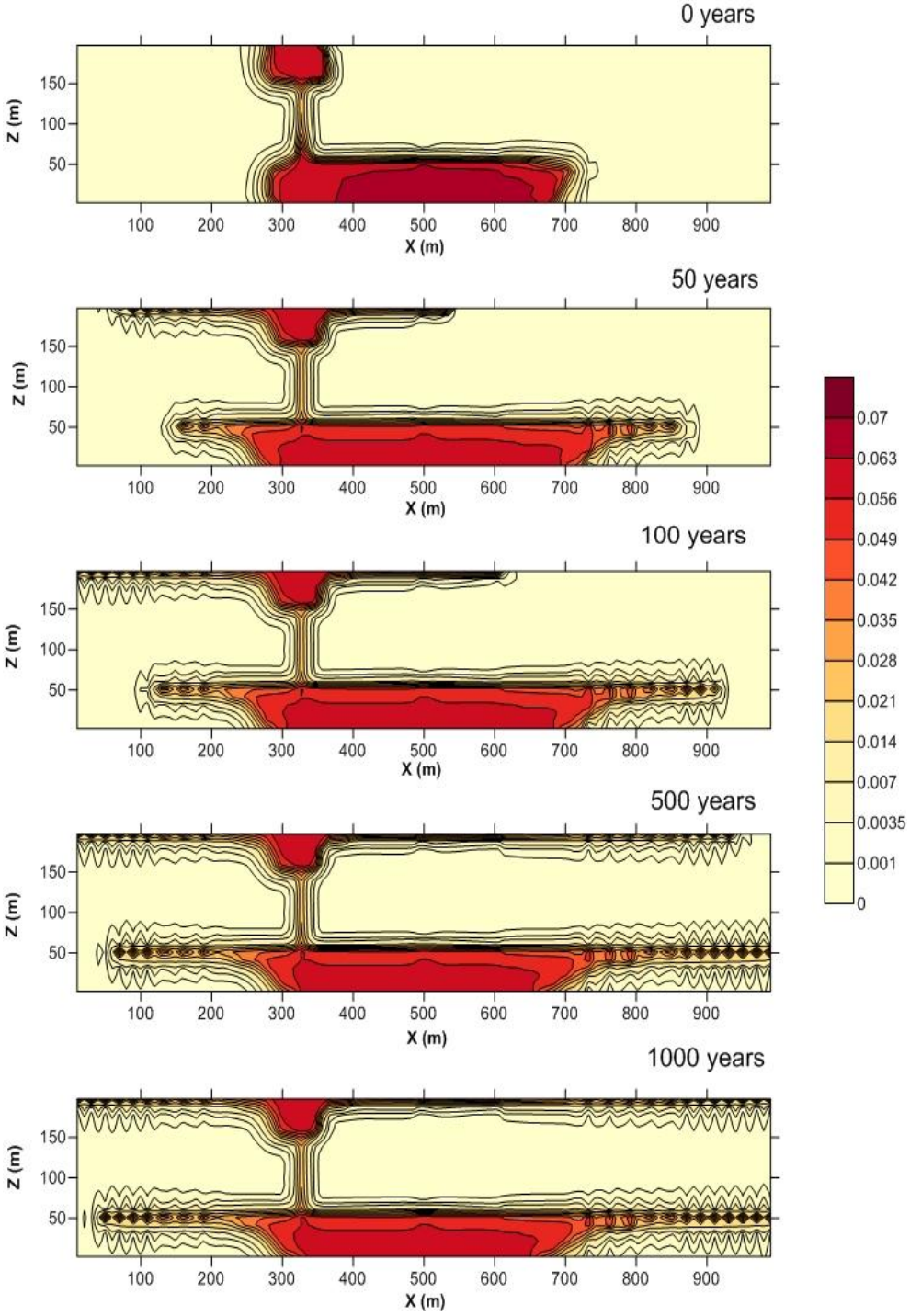

Fig. 16. Mass fraction of CO_2 in the water (XCO_2L) in the system with a fractured zone (Base Scenario) simulated from the end of the injection until 1,000 years later

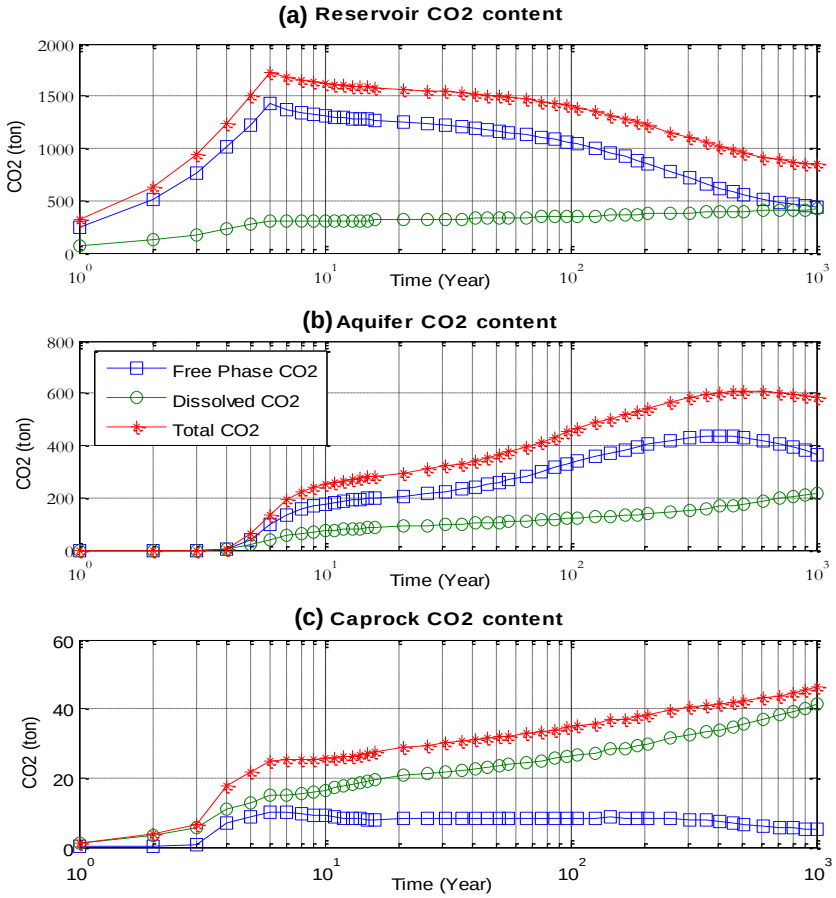

Fig. 17. CO_2 phase mass (Total, free and dissolved) for the Base Scenario in the a) Reservoir, b) Aquifer and c) Caprock.

There are two steps for dissolved CO_2; the first step is in the injection period, and the second step occurs after the injection, in which dissolved CO_2 is continually increased over a logarithmic time scale (Fig. 17.a).

The total amount of CO_2 that is leaked from the reservoir into the aquifer layer through the fracture zone has a similar shape as the free-phase CO_2. Carbon dioxide enters into the aquifer four years after injection and increases at a high rate for 10 years, after which CO_2 increases until 400 years, and then starts to decline (Fig. 17.b).

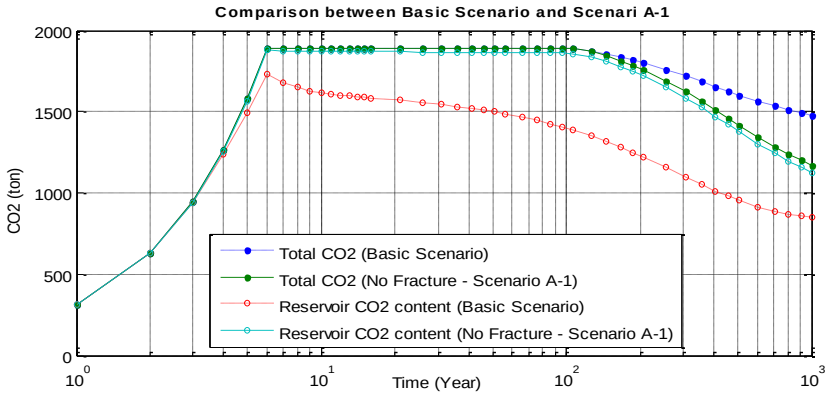

Fig. 18. CO_2 mass in the basic scenario and Scenario A-1 for the entire system and the reservoir layer.

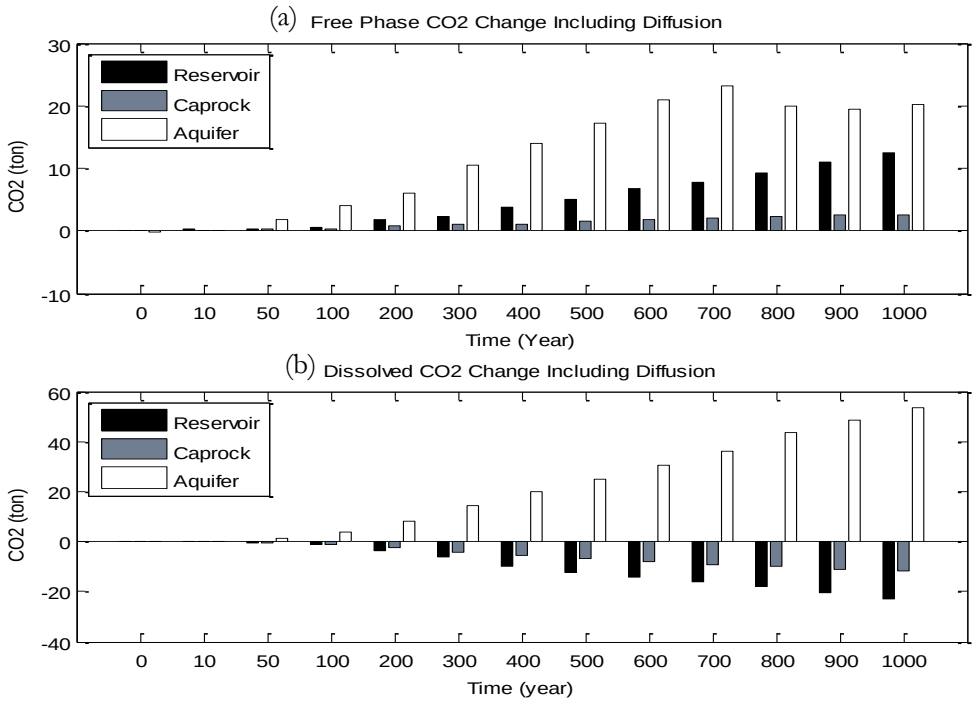

Fig. 19. Mass change of CO_2 phases when including diffusion in the simulation. (a) free- phase CO_2; (b) dissolved CO_2.

The results in Fig. 17.c indicate that most of the CO_2 in the caprock is in the dissolved phase. However, in the reservoir and aquifer layers, the there is more CO_2 in the gas phase than in the dissolved phase. The CO_2 in the gas phase leaks through the fracture zone for 3 years after injection. The amount of free CO_2 begins to decrease when CO_2 injection has stopped.

Comparing the base scenario and scenario A-1 (which does not include a fracture zone in the caprock) (Fig. 18) shows that in the case of Scenario A-1, there is a small difference between the total CO_2 in the system and the reservoir, but in the basic scenario, there is a striking difference between the reservoir CO_2 content and the total amount of CO_2 in the system.

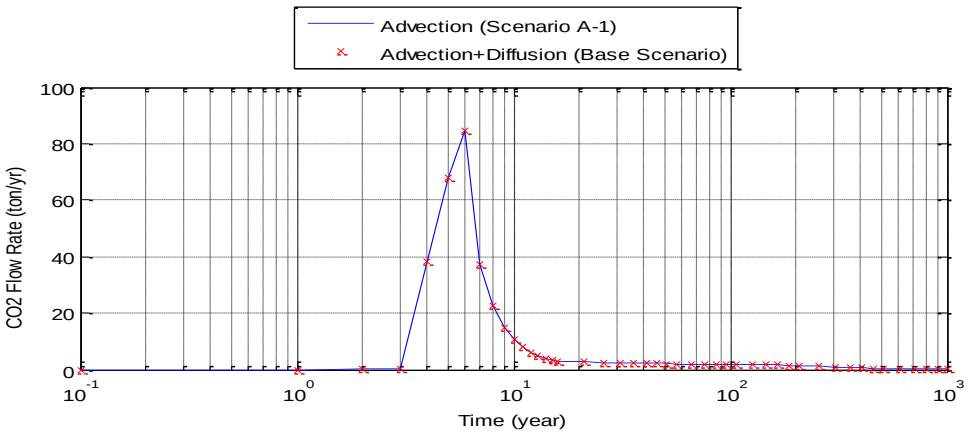

Fig. 20. CO_2 flow from the outlet of the fracture zone for the base scenario and scenario A-1.

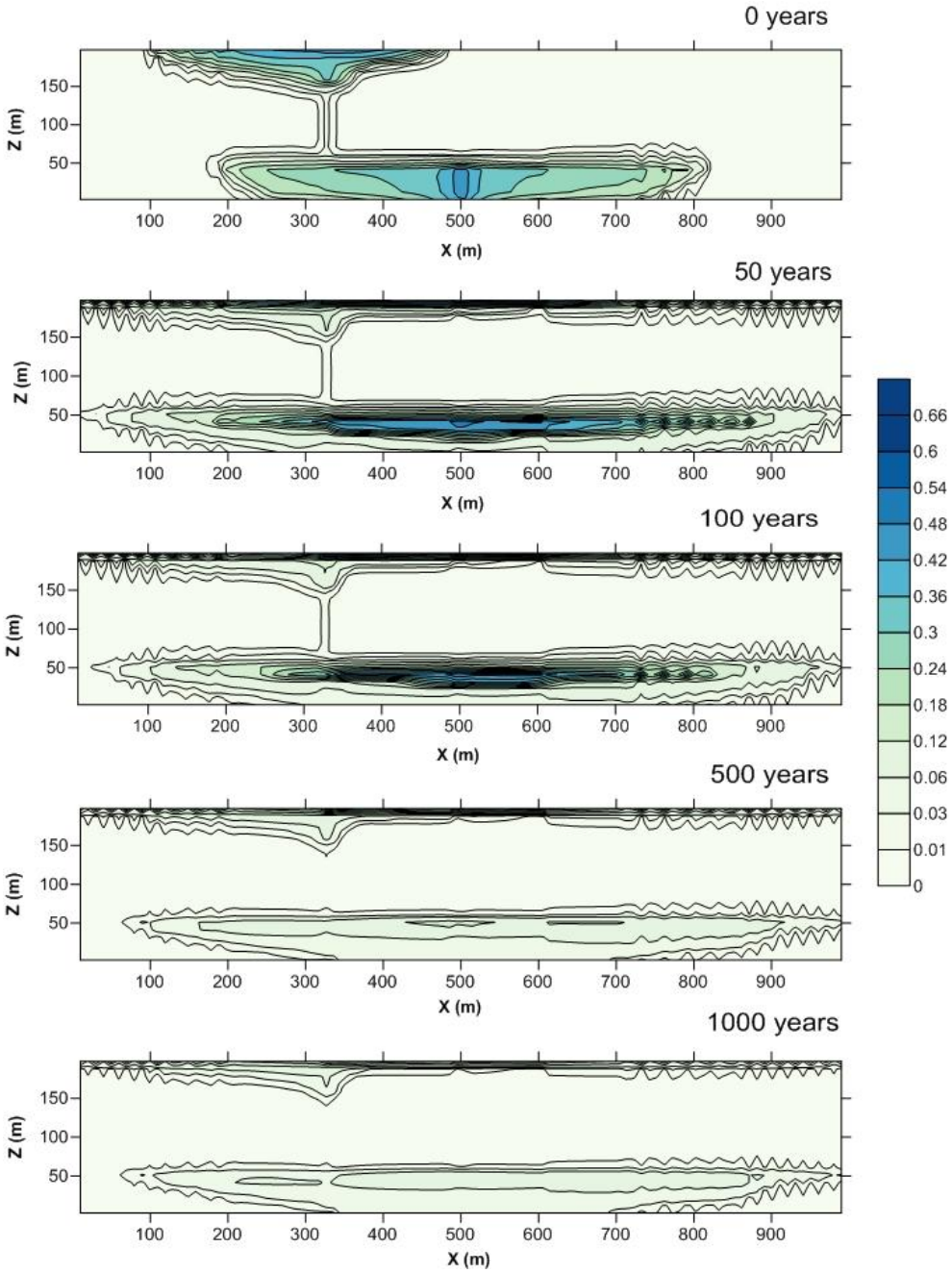

Fig. 21. Supercritical CO_2 gas phase (SG) migration in the reservoir simulated from the end of the injection period until 1,000 years later.

5.3. **Diffusion and Advection (Scenario A-2)**

Neglecting diffusion has little impact on the transport of CO_2 for both the free-phase CO_2 plume and the transport of dissolved CO_2 in the aqueous phase. However, including diffusion processes causes a different influence on the CO_2 phases in the different layers of the system (Fig. 19).

For free-phase CO_2 or the gas phase, including diffusion increases the amounts of CO_2 in the various layers over time (Fig 19.a). At the end of the 1,000-yearperiod, the percentage of free-phase CO_2 increases in the reservoir and is approximately 2.807%, which is minor compared with the total mass of CO_2 in the gas phase. For the aquifer, the CO_2 amount increases to 5.223%, and it is approximately 20 tons. For the caprock, a

significant change occurs; the total increase in CO_2 is approximately 33.85%, which is approximately 2.55 tons of free CO_2. For dissolved CO_2, including diffusion has different effects on the different layers (Fig 19.b). For the caprock and the reservoir, dissolved CO_2 decreases; in contrast, dissolved CO_2 increases for the aquifer. Here, at the end of the 1,000-year period, the amount of dissolved CO_2 reduction in the reservoir is approximately 5.85 tons, which is twice the free-phase CO_2. For the caprock, similar to free-phase CO_2, the dissolved CO_2 amount decreases by 39.7%, which is approximately 11.74 tons. For the aquifer layer against the two previous layers, the amount of dissolved CO_2 increases by 24.81% or approximately 54 tons. Comparing the two scenarios at the end of 1,000 years, the total CO_2 in the system domain increases by approximately 53.2 tons or 3.74%.

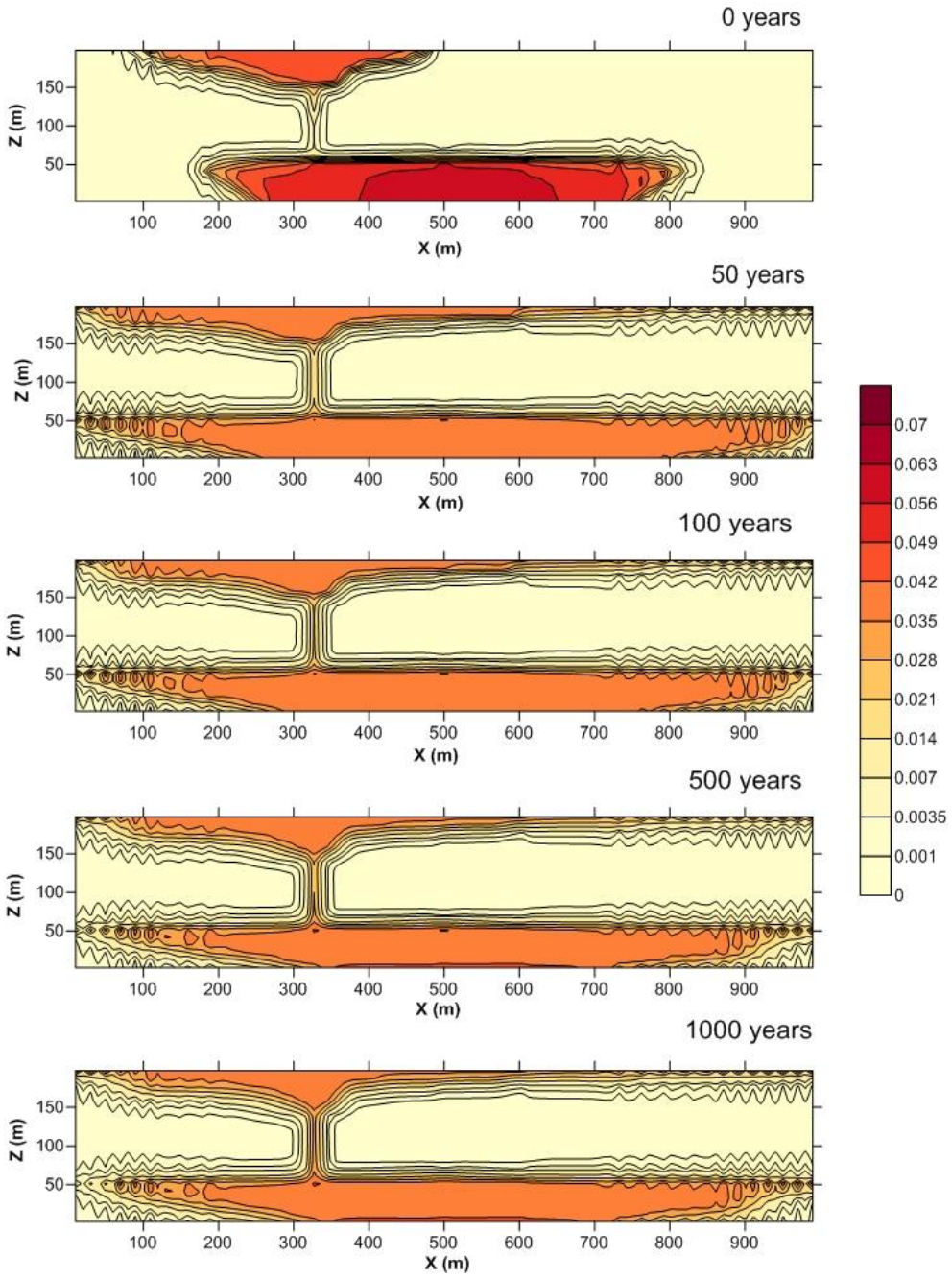

Fig. 22. Mass fraction of CO_2 in the water (XCO_2L) simulated from the end of the injection period until 1,000 years later.

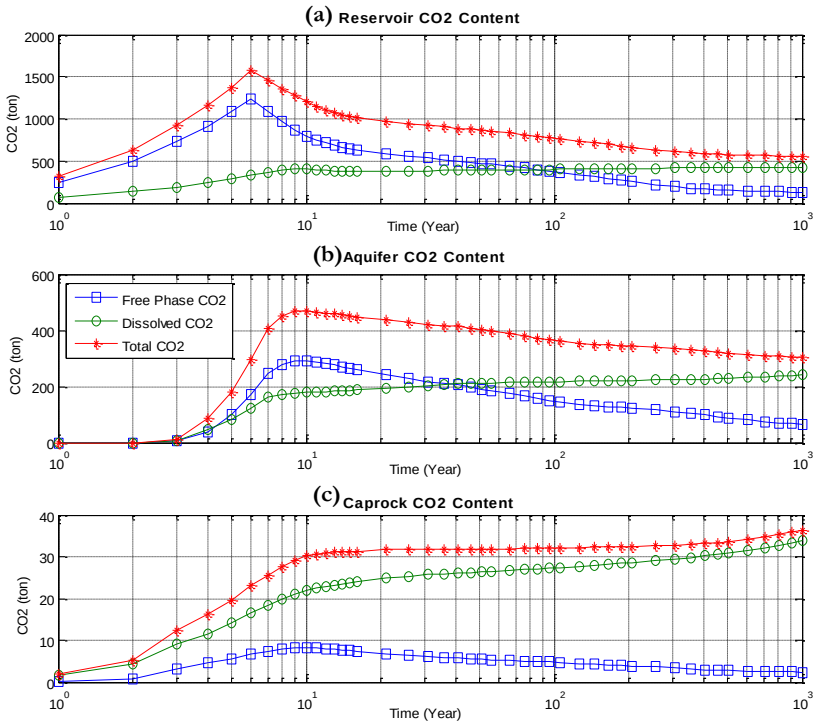

Fig. 23. CO_2 phase mass (Total, free and dissolved) in the a) Reservoir, b) Aquifer and c) Caprock for Scenario A-3.

The maximum flow rate from the fracture outlet at the aquifer layer occurs at the end of the injection period. It then starts to decrease sharply five years later (Fig. 20). Twenty years after injection, the rate of CO_2 flow from the outlet drops greatly. Over the passage of time, the rate of CO_2 flow with a low slope decreases such that after 1,000 years, it is close to zero. Thus, considering diffusion does not influence the flow rate, and in both scenarios, the curves of CO_2 flow rate are matched over the entire 1,000 years.

5.4. Reservoir Depth (Scenario A-3)

As discussed above, the physical properties and transport of CO_2 are dependent on pressure. Finding an appropriate CO_2 sequestration site and reservoir depth is a function of pressure. Reservoir temperature is also a function of reservoir depth. However, in this study, to simplify the problem, the reservoir temperature is assumed to be the same as in the base scenario.

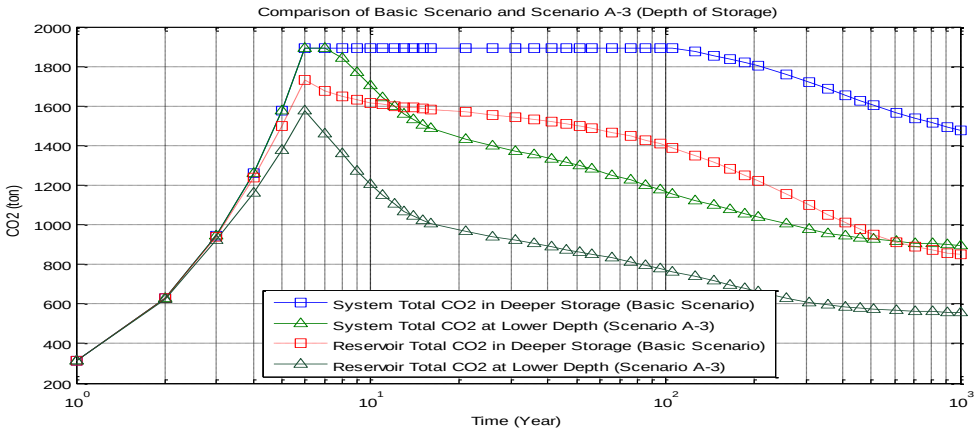

Fig. 24. CO_2 mass in the Base Scenario and Scenario A-3 for the entire system and reservoir layer

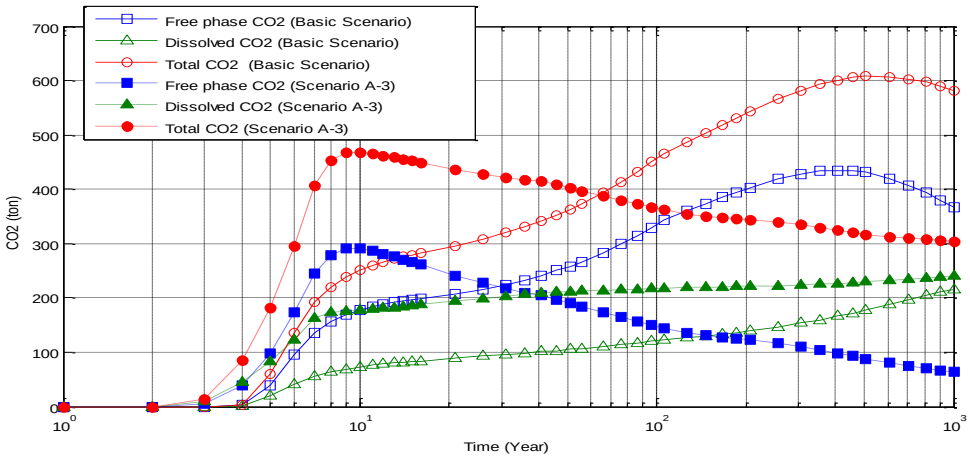

Fig. 25. Comparison of the CO_2 mass in different phases between the Base Scenario and Scenario A-3 for the Aquifer layer

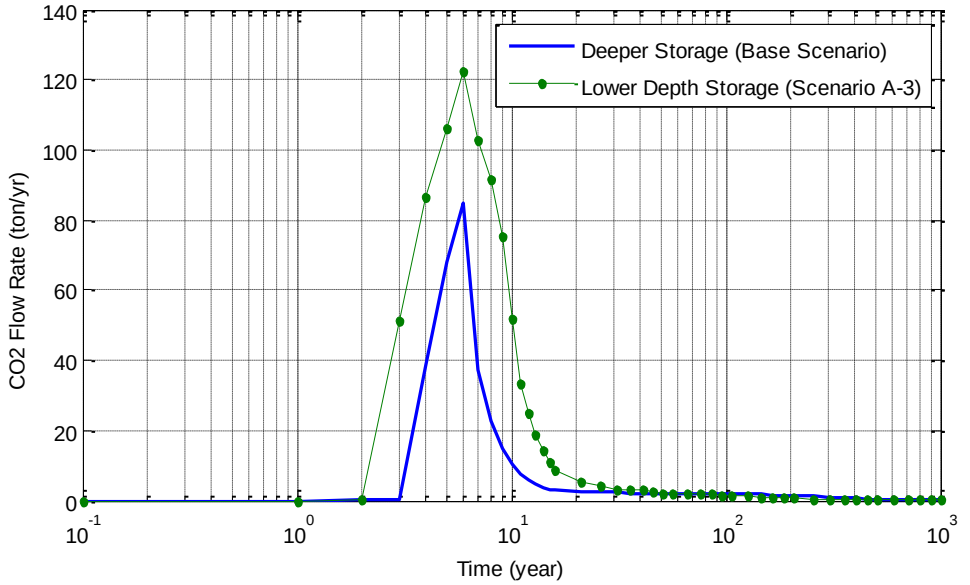

Fig. 26. CO_2 flow from the outlet of the fracture zone for the Base scenario and Scenario A-3.

In a shallower reservoir, pressure is decreased. The influence of this pressure reduction on free-phase CO_2 or the CO_2 plume in the system is significant (Fig. 21). CO_2 in the gas phase in this scenario is spreading faster than in the basic scenario. Here, after 50 years of injection, the CO_2 moves out of the left and right boundaries, an event that took over 500 years in the basic scenario years (Fig. 15).

For the aqueous phase with dissolved CO_2 (Fig. 22), the mass fraction is smaller than in the base scenario (Fig. 16). As in the basic scenario, the dispersion of dissolved CO_2 is similar to the gas phase. The CO_2 plume is dispersed over approximately 700 m in the reservoir layer. In the aquifer layer, CO_2 is dispersed approximately 500 m. Compared with the base scenario, in the reservoir CO_2 mass fraction extended 400 m more; in the aquifer layer, it extended equally.

The CO_2 mass balance in each layer for the different phases shows the influence of pressure reduction on CO_2 transport and leakage (Fig. 23). In the reservoir layer, after 1,000 years, more CO_2 is in the dissolved phase than as free-phase CO_2 (Fig. 23a). Moreover, in the aquifer layer, most of the CO_2 is dissolved after 1,000 years (Fig. 23.b). In the caprock, dissolved CO_2 predominates.

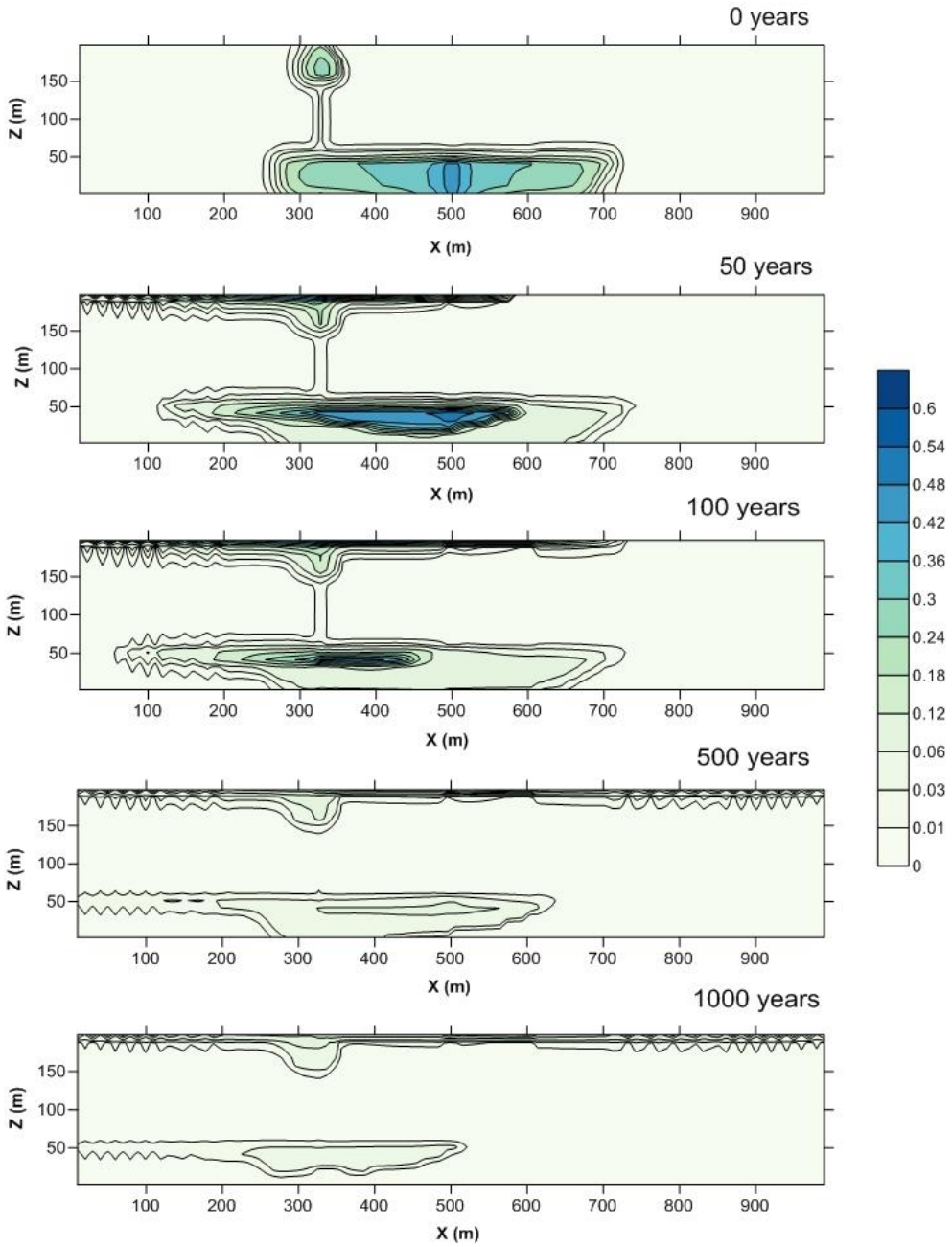

Fig. 27. Supercritical CO_2 gas phase (SG) migration in the system with groundwater flow in the reservoir layer (Scenario A-4) simulated from the end of the injection period until 1,000 years later.

The free-phase CO_2 in the reservoir has four stages. The first stage is in the injection period, after which the total amount of CO_2 in the system is approximately 1,893.5 tons, of which 83.15% (1,574.5 tons) is in the reservoir. The next stage occurs 15 years after the injection, in which the total CO_2 is approximately 1,432.8 tons, 67.4% of which is in the reservoir. The third stage is between 15 and 120 years, and the total CO_2 is 1,123.8 tons, of which 65.7% is in the reservoir. The final stage is at 1,000 years, in which the amount of CO_2 is 896.6 tons, of which 62% is in the reservoir. The dissolved CO_2 stages in the reservoir are different than for free gas and generally can be divided into two stages, one of which is within the first 10 years and the second of which is during the following 1,000 years. The first stage has a higher rate of dissolution, but in the second stage, the rate of dissolution is nearly constant.

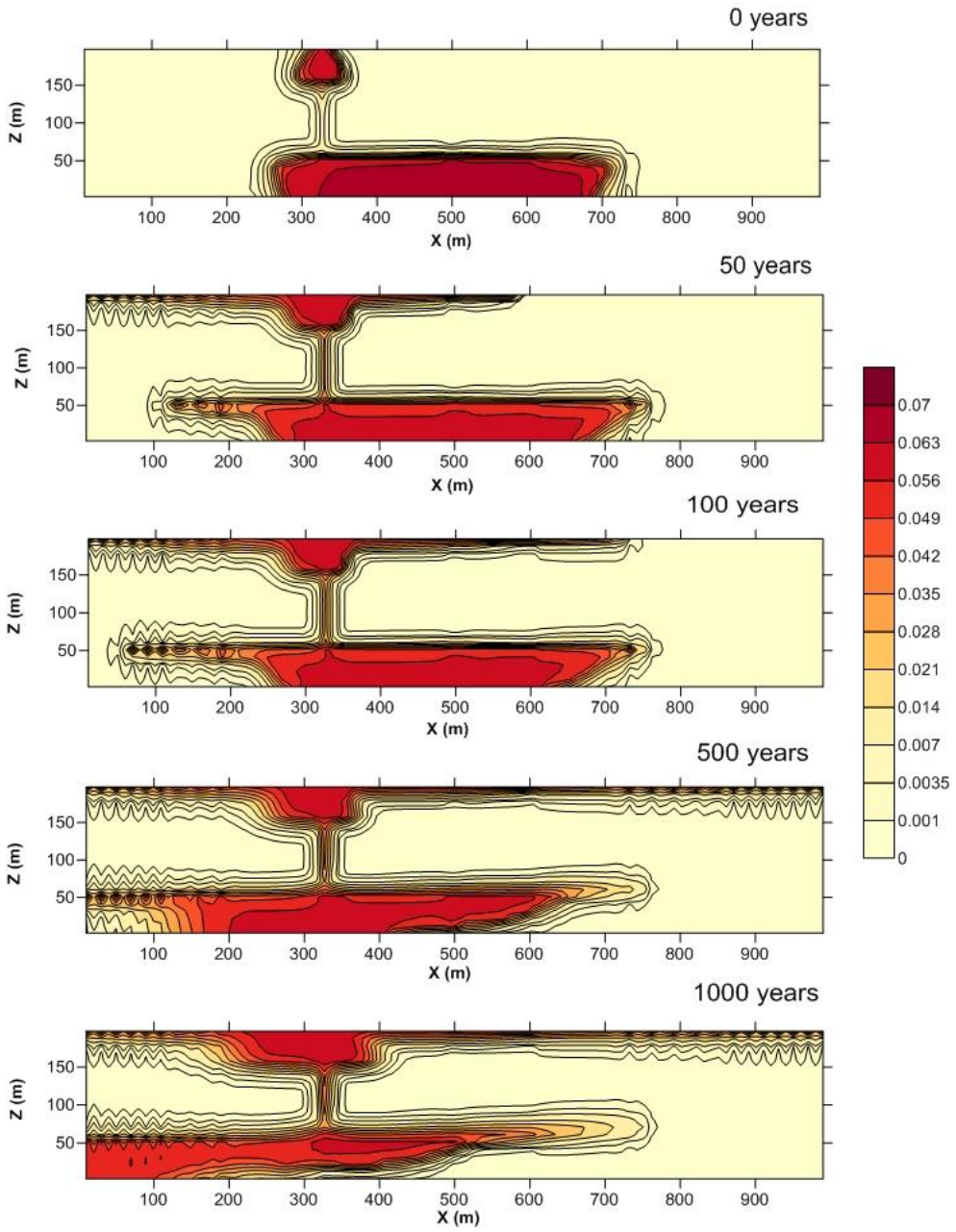

Fig. 28. Mass fraction of CO_2 in the water (XCO_2L) in the system with groundwater flow in the reservoir layer (Scenario A-4) simulated from the end of the injection period until 1,000 years later.

In the aquifer layer, the simulation shows a similar behavior as the reservoir, and the only difference is a three-year lag time; the maximum amount of CO_2 in the aquifer is approximately 468.8 tons ten years after starting the injection. The caprock total CO_2 amount is relatively low compared with that in the aquifer and reservoir, although it is still of value to know how much CO_2 is trapped at the caprock.

The total amount of CO_2 1,000 years after injection is 36.4 tons. A comparison between the Base Scenario and Scenario A-3 shows the importance of reservoir depth in the total amount of leakage and transport in the system (Fig. 24). The total amount of CO_2 that remains in the system with the shallower storage is greatly reduced with time compared with the Base Scenario. The behavior of total CO_2 in the reservoir is also different. In scenario A-3, CO_2 in the gas phase has a

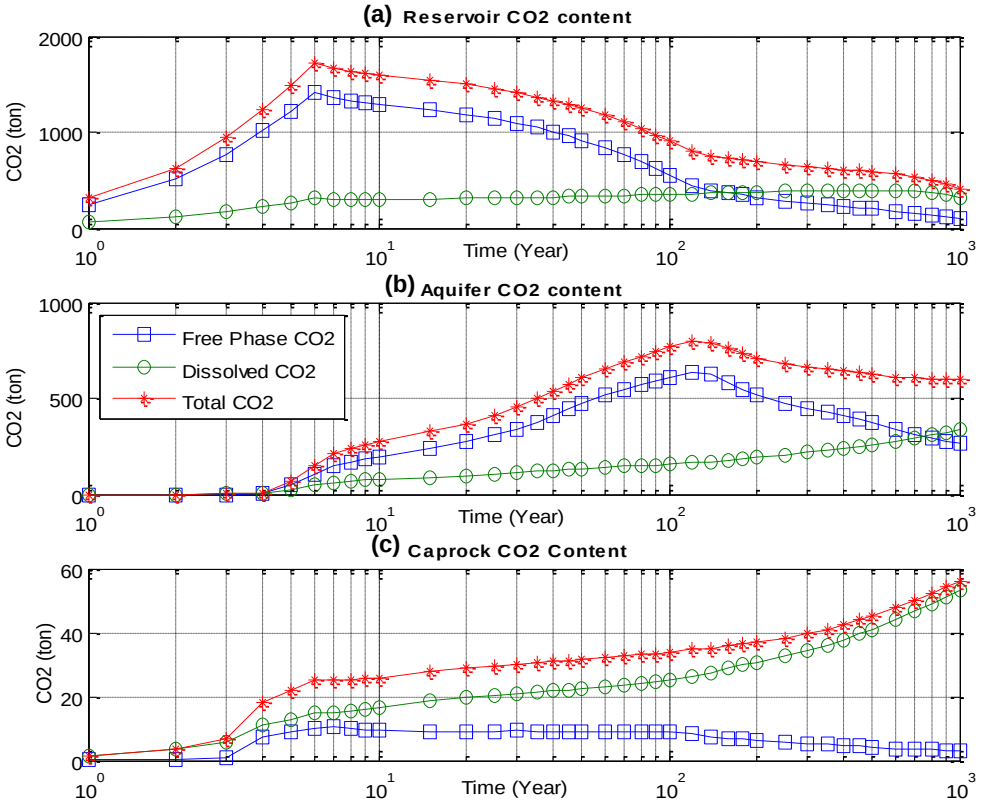

Fig. 29. CO_2 phase mass (Total, free and dissolved) in the a) Reservoir, b) Aquifer and c) Caprock for Scenario A-4.

nearly constant distance with total CO_2 in the system, but for the Base Scenario, the pattern differs between the system and reservoir CO_2 amounts. In the aquifer layer, there are completely different patterns between the basic and A-3 scenarios.

The free-phase CO_2 in the Scenario A-3 is reduced after the injection period (which does not occur in the Base Scenario), and it is reduced after 500 years. The dissolved CO_2 in both scenarios is increased, but in the case of scenario A-3, more dissolution occurs during injection, and the rate of dissolution after injection is lower than in the Base Scenario. The important point in the aquifer layer is that the amount of CO_2 that is leaked into the aquifer a few years after the injection period is greater than in the Base Scenario (Fig. 25).

In the aquifer, by reducing the depth of storage, the amount of CO_2 in both the free and dissolved phases is greater after the first 10 years, after which the amounts of CO_2 start to decline. Using the flow rate of CO_2 from the outlet of the fracture can help identify the reason for this large change in CO_2 phase behavior (Fig. 26). The flow rate of CO_2 in the outlet of the fracture with a lower depth occurs earlier and at a higher amount than in the Base Scenario. The peak value for the CO_2 flow rate in Scenario A-3 is approximately 122 tons/yr, and this value is approximately 84 tons/yr for the Base scenario and has continued for 14 years after peak flow.

5.5. Groundwater Flow in the Reservoir (Scenario A-4)

Groundwater flow in the reservoir layer influences both the transport of the CO_2 plume in the system and the leakage percentage. CO_2 in the

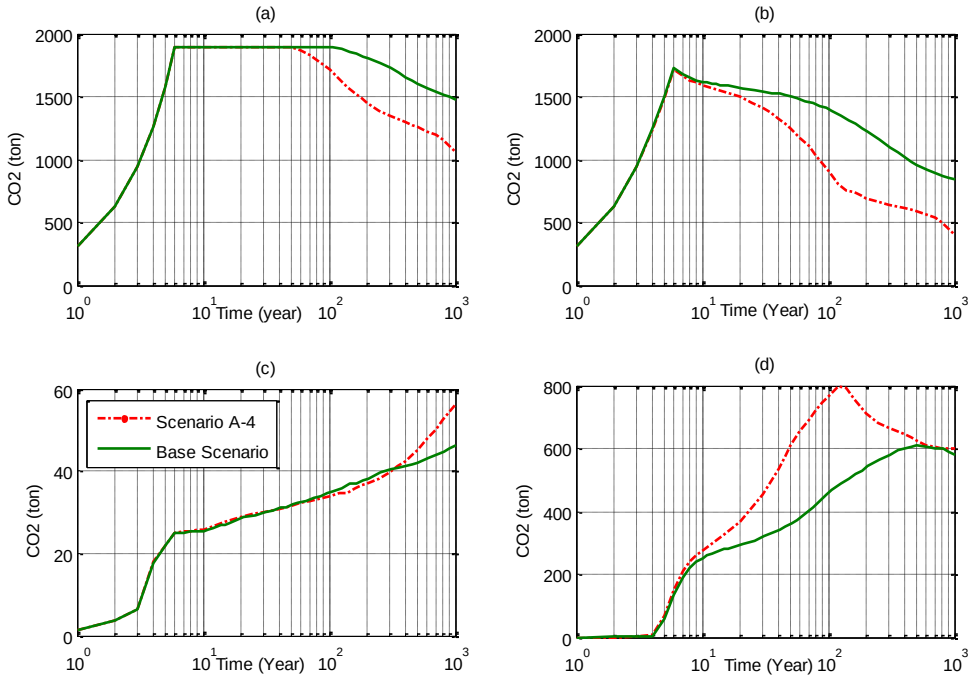

Fig. 30. Comparison between scenario A-4 and the Base Scenario for the total amount of CO_2 in the (a) All System Domain, (b) Reservoir, (c) Aquifer and (d) Caprock.

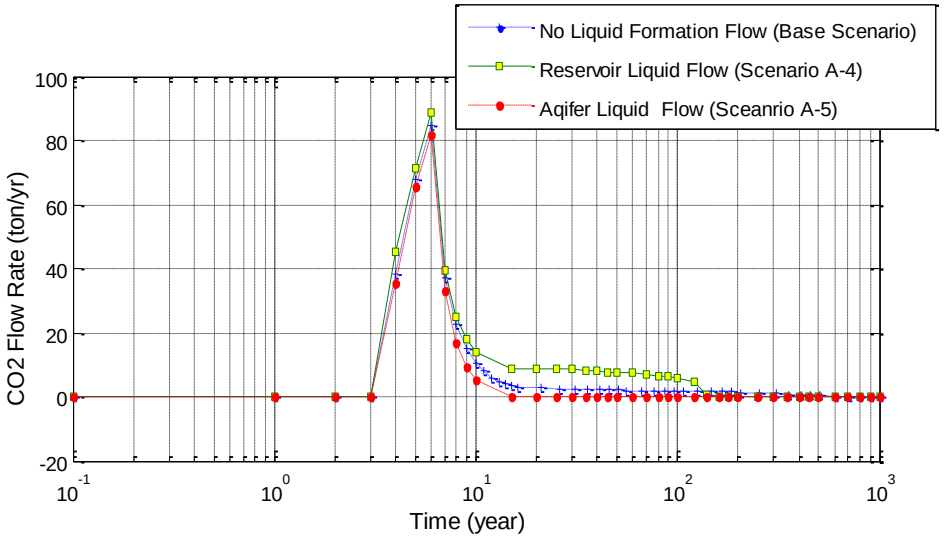

Fig. 31. CO_2 flow from the outlet of the fracture zone for the Base scenario and Scenarios A-4 and A-5.

reservoir moves with the groundwater direction (Fig. 27). The expansion of free-phase CO_2 and dissolved CO_2 in the groundwater flow direction does not affect the shape of the CO_2 plume in the aquifer layer or the caprock layer (Fig. 28). The general behavior of CO_2 in the various layers is similar to the base scenario (Fig. 29). In the reservoir layer, free-phase CO_2 peaks at the end of the injection period, then has a higher rate until 100 years compared with the rate of reduction until 1,000 years (Fig 29.a). For dissolved CO_2, after a higher rate of dissolution, it increases slowly until 1,000 years. Compared with the Base Scenario, in the aquifer layer, the peak CO_2 mass content occurs earlier, and after

100 years, the CO_2 starts to decline. The dissolved CO_2 in the aquifer increases over time such that at the end of 1,000 years, the amount of dissolved CO_2 is higher than the amount of free-phase CO_2 (Fig. 29.b). In the case of the caprock, the basic pattern is similar to the Base scenario, and most of the CO_2 that is present at the caprock is in the dissolved phase, and the rate of the gas phase decreases over time (Fig. 29.c).

A comparison between the Base Scenario and Scenario A-4 (groundwater flow in the reservoir layer) (Fig. 30) shows that the total amount of CO_2 in the system domain in scenario A-4 is less than in the base scenario after 50 years. In the reservoir layer, the total amount of CO_2 begins to decrease after the injection period. The maximum difference between the CO_2 amounts in the reservoir occurs after 120 years, and after this time, the difference in CO_2 amounts decreases (Fig. 30.a). In the aquifer layer, at the end of 1,000 years, both scenarios

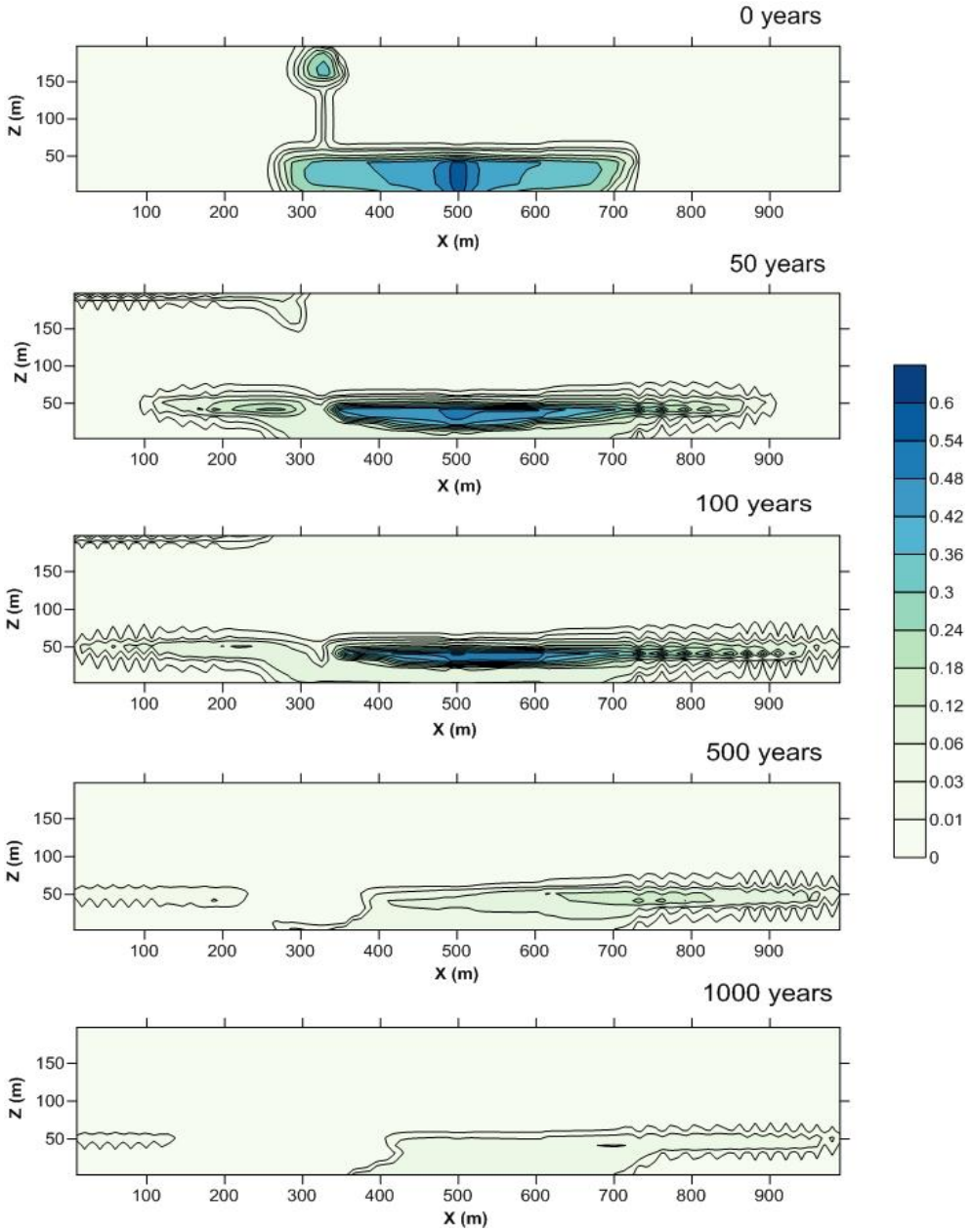

Fig. 32. Supercritical CO_2 gas phase (SG) migration in the system with groundwater flow in the reservoir layer (Scenario A-4) simulated from the end of the injection period until 1,000 years later.

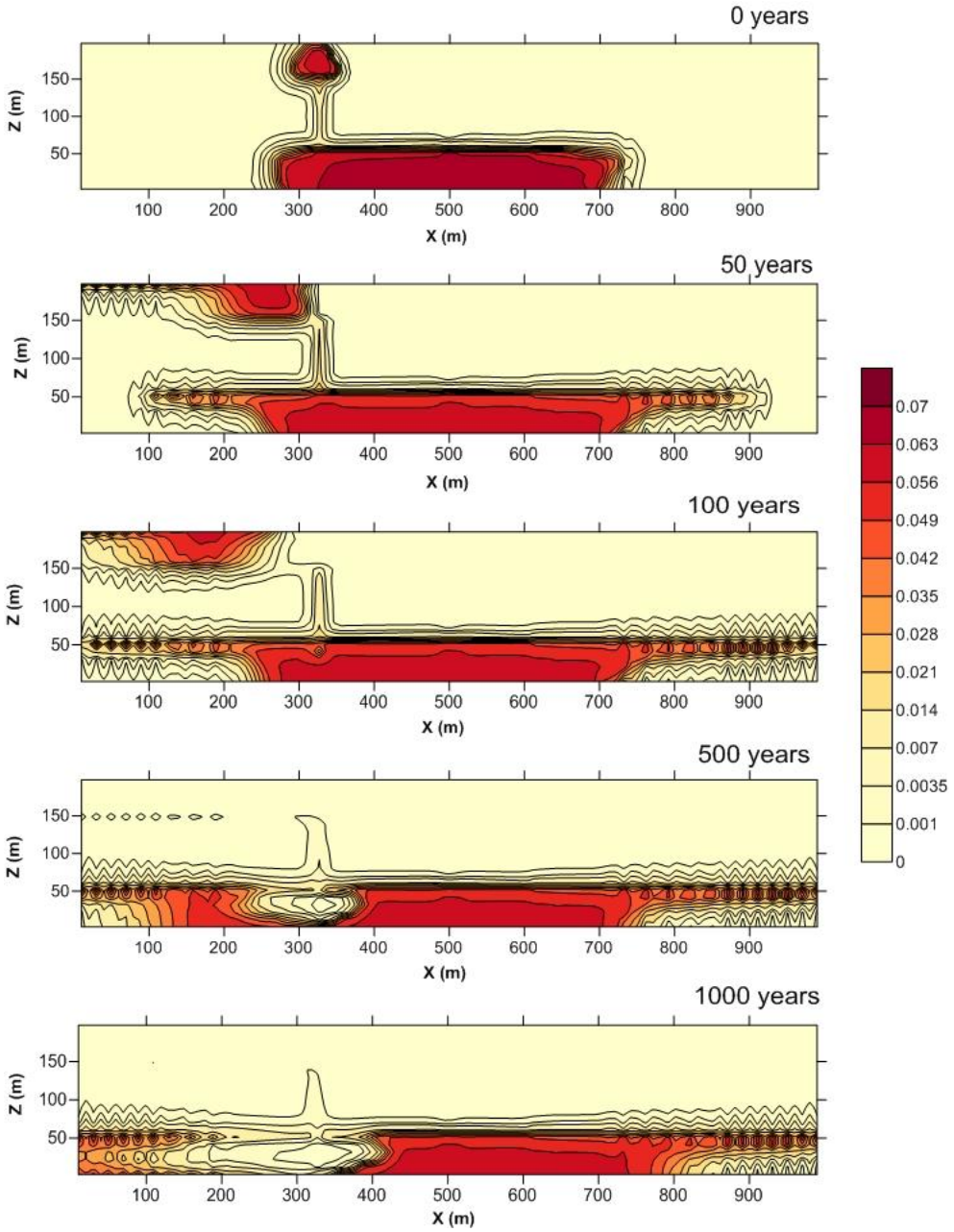

Fig. 33. Mass fraction of CO_2 in the water (XCO_2L) in the system with groundwater flow in reservoir layer (Scenario A-4) simulated from the end of the injection period until 1,000 years later.

have the same amount of CO_2 despite following different paths (Fig. 30.c).

The total amount of CO_2 in the aquifer in scenario A-4 is higher than in the base scenario between the end of the injection period and 500 years; after this, the two scenarios have the same amount of CO_2. In the caprock, before 250 years, the two curves are similar; however, after that time, the amount of CO_2 in the base scenario becomes smaller than in scenario A-4.

The CO_2 flow rate at the outlet of the fracture for Scenario A-4 barely differs from the Base Scenario before 8 years; however, after that time, the flow rate in the reservoir with reservoir liquid flow has a higher rate, and after 150 years, this rate decreases and even becomes smaller than in the Base Scenario (Fig. 31).

5.6. **Groundwater Flow in the Aquifer Layer (Scenario A-5)**

Fifty years after the injection period, the presence of aquifer liquid flow leads to no CO_2 leakage into the aquifer layer (Fig. 32). In the presence of aquifer flow, the CO_2 plume moves to the right, and the accumulation of single-phase CO_2 under the facture is zero after 500 years.

For dissolved CO_2, the CO_2 fraction in the aqueous phase under the fracture is approximately after 500 years, and the mass fraction of CO_2 in the aqueous phase in the aquifer layer is approximately zero after 500 years (Fig. 33). To provide a better representation, the CO_2 mass balance for the various layers in this scenario is shown in Fig. 34.

For this scenario, the difference between the mass balance curves for the aquifer layer and the reservoir and caprock is similar to the base scenario. Single-phase CO_2 in the aquifer is increased 10 years after the injection has started. After that time, the level begins to decline, and after 300 years, it reaches zero (Fig. 34.b). Dissolved CO_2 starts to increase due to free-phase CO_2 entering the aquifer. The dissolved CO_2 begins to decline sharply by 100 years after the injection starts. The maximum amount of CO_2 that enters the aquifer is approximately 230 tons, and this amount is present in the aquifer from 10 to 40 years after the injection has started. In this scenario, the maximum amount of CO_2 in the reservoir and caprock is approximately 1,740 and 32.1 tons, respectively. A comparison of the Base Scenario and Scenario A-5 shows that the total CO_2 in Scenario A-5 in the reservoir and caprock differs little from the Base Scenario. However, in the aquifer, there is a large difference that starts at the end of the injection period. The total amount of CO_2 in the system is different after 100 years (Fig. 35). An examination of the CO_2 flow rate at the outlet of the fracture for this scenario (Fig. 32) shows that, in this scenario, after 15 years, the flow rate becomes zero or flow moves in the opposite direction. However, for 15 years after the injection period, the flow curve is similar to base scenario.

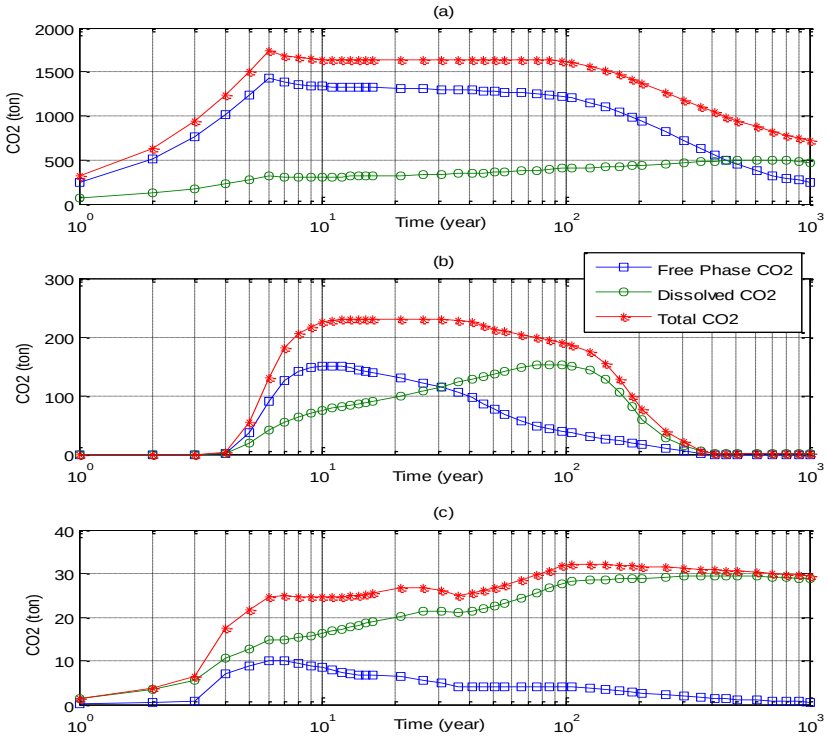

Fig. 34. CO_2 phase mass (Total, free and dissolved) in the a) Reservoir, b) Aquifer and c) Caprock.

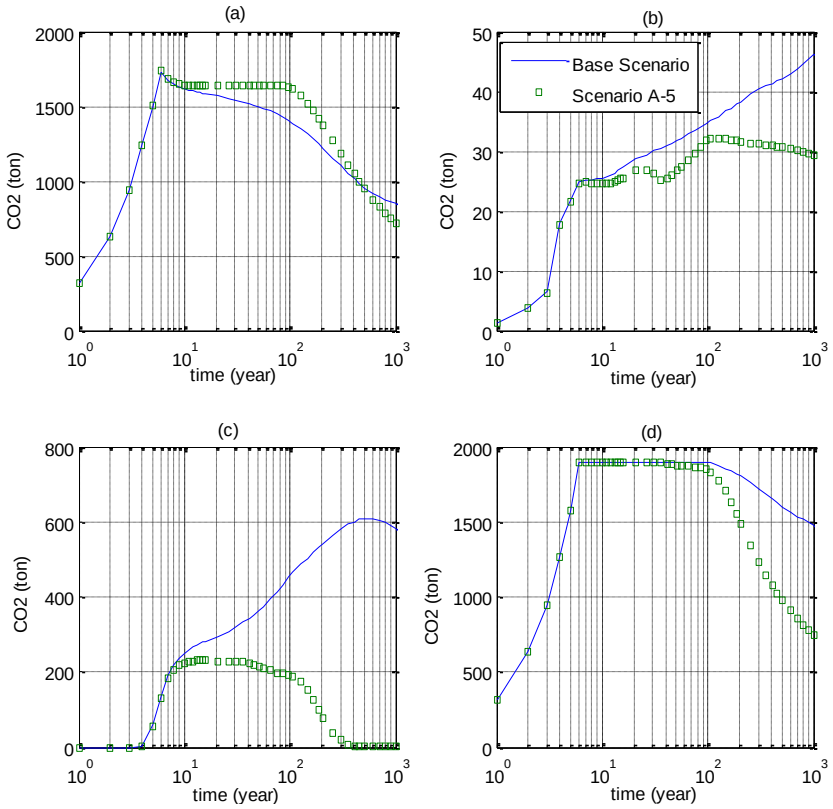

Fig. 35. Comparison between scenario A-5 and the Base Scenario for the total amount of CO_2 in (a) All System Domains, (b) the Reservoir, (c) the Aquifer and (d) the Caprock.

5.7. **Salinity of the Formation Fluid (Scenario A-6)**

Differences in the salinity of the formation fluid can have an influence on CO_2 sequestration. In a system with a salinity of 10 (which is equal to 10 grams of salt in 1 liter of solution), there are different phase behaviors in all of the system layers. In the reservoir layer, salinity causes an increase in the total amount of CO_2 in the system. In addition, the values of dissolved and free-phase CO_2 also increase. After 1,000 years, the amount of CO_2 in all of the phases becomes equal for both scenarios (Fig. 36.a).

In the aquifer layer, there is a different result than in the reservoir. The total amount of CO_2 associated with saline water for a period of 15 years is larger than for pure water, after which the total CO_2 level stays constant; after 200 years, the level reduces, which is different than in the Base Scenario. This trend is repeated for free-phase CO_2. The amount of dissolved CO_2 in an aquifer with brine is less than in pure water (Fig. 36.b). For the caprock, the result is similar to the aquifer layer, and the salinity of water causes a drop in CO_2 amounts in all phases (Fig. 36.c).

The CO_2 flow rate from the outlet of the fracture in the saline aquifer (ScenarioA-6) shows a higher value from year 3 to year 6 after the injection period (Fig. 37). However, after this time, the two curves are briefly matched; from year 10, the curve of the pure water has a higher flow rate. The presence of such differences between these two scenarios is not distinguishable in terms of the contour plots for single-phase and aqueous phase CO_2 with respect to the dissolved CO_2 (Appendix III).

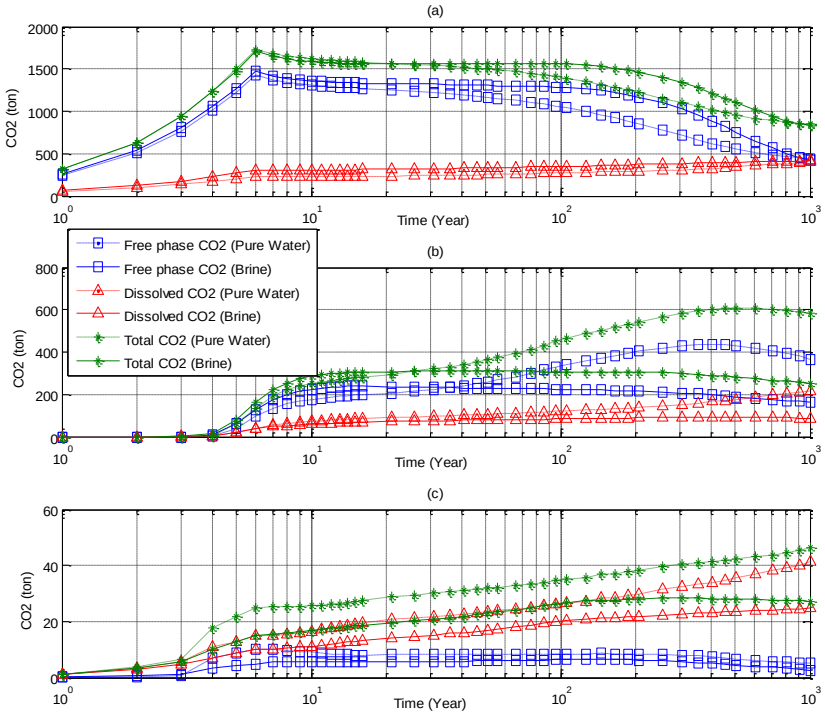

Fig. 36. Comparison between scenario A-6 and the Base Scenario for the total amount of free-phase CO_2 and dissolved CO_2 in the (a) Reservoir and (b) Aquifer.

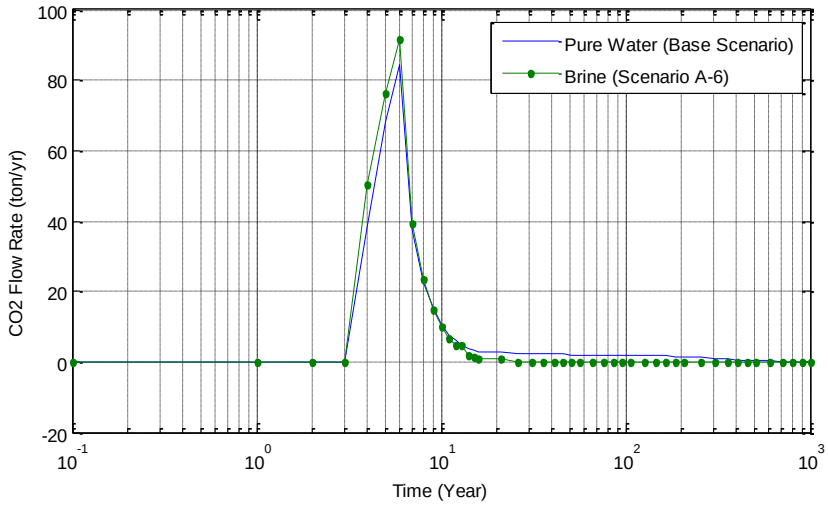

Fig. 37. CO_2 flow from the outlet of the fracture zone for the Base scenario and Scenario A-6.

5.8. Fracture Modeling Approach (Scenarios A-7 and A-8)

Using different approaches to model a fracture can change the mass balance in the system domain. Because the contour plots for single-phase CO_2 and the CO_2 mass fraction in the aqueous phase cannot represent differences between the scenarios for the fracture modeling approach (Appendix III), only the mass balance and flow from the fracture outlet are used. A comparison of the CO_2 phase diagram from the equivalent porosity method (EPM) and the multiple interacting continua (MINC) method shows differences in the aquifer and caprock CO_2 contents (Fig. 38). In the caprock layer, there is a large difference between the two

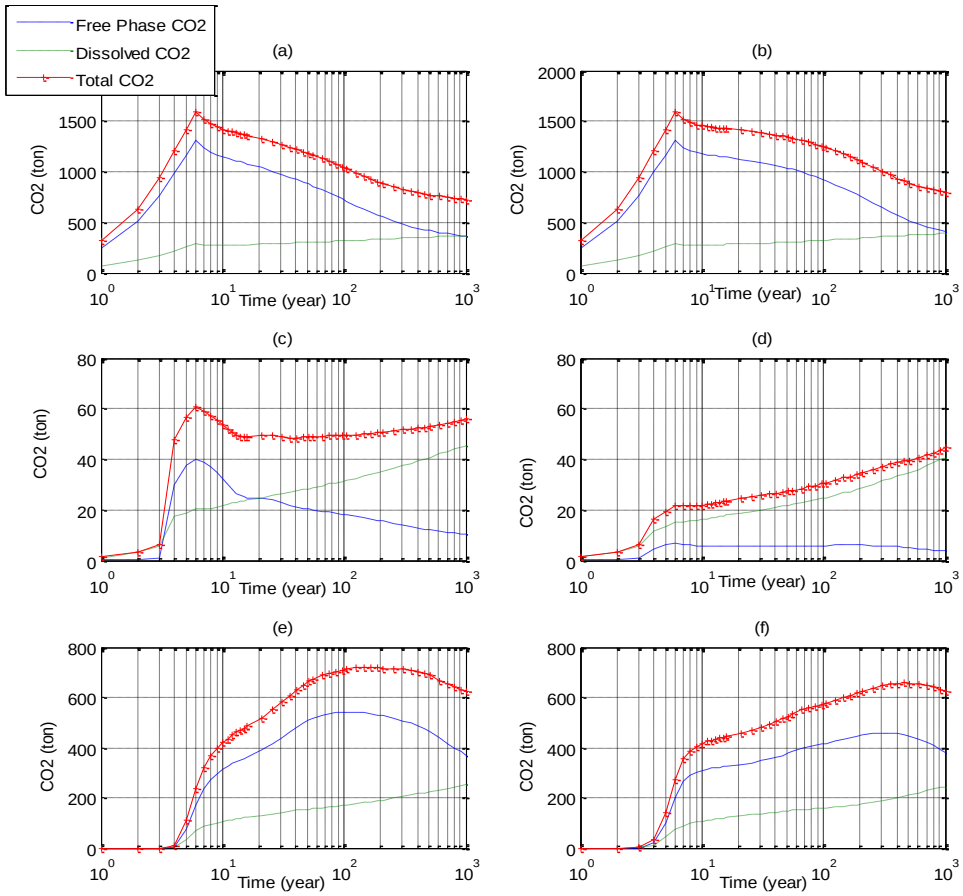

Fig. 38. CO_2 phase mass (Total, free and dissolved) in the (a) Reservoir-EPM, (b) Reservoir-MINC, (c) Aquifer-EPM, (d) Aquifer-MINC, (e) Caprock-EPM and (f) Caprock-MINC.

approaches. For the aquifer layer, the difference is apparent after year 10, and the EPM shows higher values of CO_2 in the aquifer layer. However, for the reservoir, there is no difference between the domains. To understand better the influence of the fracture modeling approaches, the effects of all of the approaches on CO_2 total mass contents in all of the layers are compared (Fig. 39).

For all of the systems, all of the approaches have a similar curve. However, it is possible to as certain that after 100 years, the CO_2 in the Dual-Porosity method is more than in the MINC method, which is more than with an equivalent method (Fig. 39.d). For the aquifer layer, there is a higher level of CO_2 using the EPM after the injection period, the MINC and dual porosity methods show smaller amounts of CO_2 during all 1,000 years. Accordingly, in the reservoir layer, the opposite behavior than that seen in the aquifer layer can be observed.

For the caprock layer, the EPM shows a higher content of CO_2, after which the Dual-porosity method shows more CO_2. However, the difference between MINC and Dual-Porosity methods is inconsequential. Following the CO_2 flow rate at the outlet of the fracture (Fig. 40) reveals that there is a large difference between peak values in the two last approaches with Dual-Porosity used in the Base Scenario. In the MINC curve, there are two recognizably separable behaviors. The first is before the end of the injection, where there is a higher flow rate, and the second is immediately after stopping the injection, where the flow rate drops and becomes similar to that from the dual-porosity method.

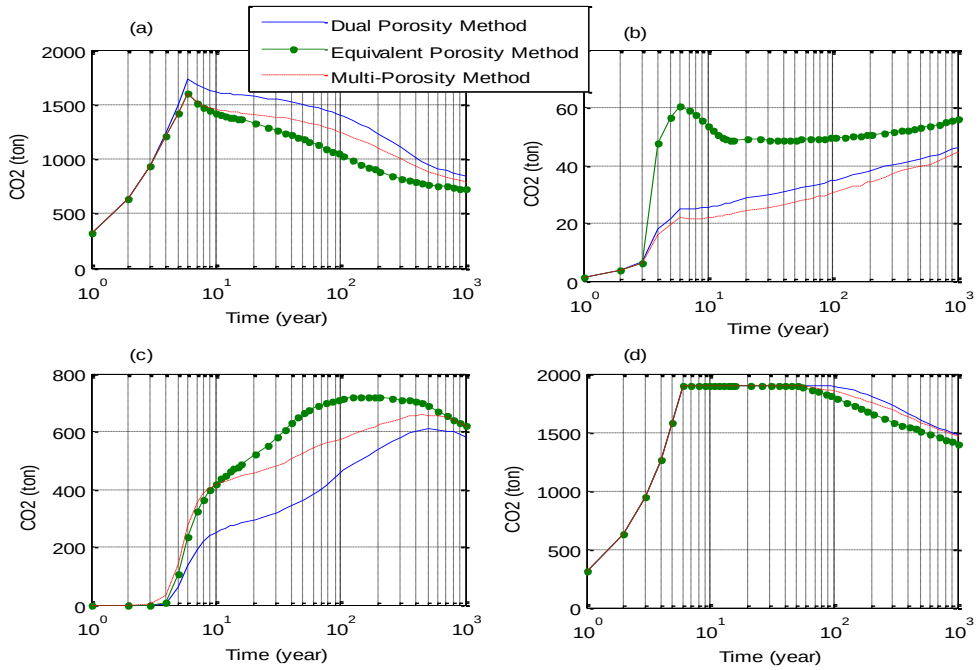

Fig. 39. Comparison between scenario A-7, Scenario A-8 and the Base Scenario for the total amount of CO_2 in (a) All System Domains, (b) the Reservoir, (c) the Aquifer and (d) the Caprock.

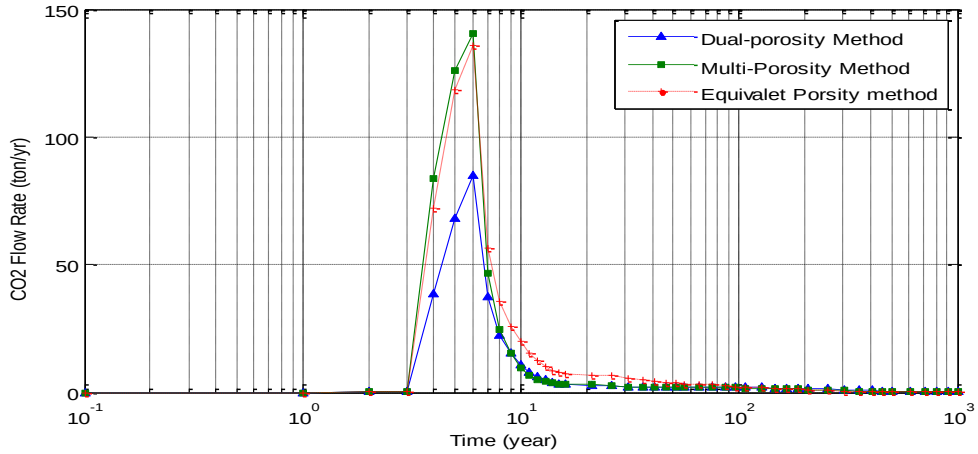

Fig. 40. CO_2 flow from the outlet of the fracture zone for the Base scenario, Scenario A-7 and Scenario A-8.

In the model using the EPC approach, the flow rate in the fracture outlet is higher than in the Base scenario both during and after the injection.

6. DISCUSSION

The main issues that can be obtained from the results section are as follows:

- The influence of the features and processes involved in CO_2 leakage (CO_2 flow rate from the fracture outlet) over the short and long terms;
- The role of a fractured caprock on CO_2 sequestration;
- Comparative analyses were applied between the alternate scenarios and the Base scenario to examine the aforementioned issues. After which, how the model can be modified is explained.

6.1. Fractured vs. Sealed Caprock

The main difference in the results of these two scenarios (i.e., the Base scenario vs. scenario A-1) was the presence of CO_2 in the aquifer layer. The presence of fractures in the caprock causes the transport of CO_2 into the aquifer layer. The existence of fractures with high permeability compared with the low-permeable caprock, and the pressure difference between the top and the bottom of the fracture, causes the transport of CO_2 into the aquifer. The primary processes of transport are advection and convection in the fracture.

The mass balance results show that after 1,000 years, there is a higher amount of CO_2 in the system with fractures. The presence of fractures is the factor that affects the CO_2 plume shape. When a fracture is present in the caprock, CO_2 moves towards it by advection. A key point for comparing these two scenarios is that the presence of a fracture increases CO_2 dissolution in the aqueous phase. The presence of a fracture causes a higher distribution of CO_2 in the gas phase of the system, which in turn leads to more dissolution.

6.2. Leakage of CO_2

The leakage of CO_2 means that CO_2 migrates across the boundary of the storage layer (Oldenburg et al., 2009). Thus, the transport of CO_2 from the reservoir layer, which is the host layer for CO_2 injection, to the aquifer layer in the top of the caprock is considered to be a leakage process. As explained previously, the leakage path is the fractured zone in the caprock. The presence of fractures with high permeability causes the CO_2 that is injected into the reservoir to move to the aquifer layer and causes the caprock to lose its trapping ability. Simulating various leakage scenarios helps us to identify the impact of each scenario on leakage amounts. The leakage of CO_2 into the aquifer layer is important in both the short and long terms.

6.2.1. *Diffusion*

The diffusion process does not have an influence on the leakage of CO_2 in the short term, which is the principal leakage component (Fig. 20). However, in the long term, the leakage rate in the Base scenario (advection and diffusion) is lower than in scenario A-2 (advection).

The main reason for the aforementioned difference is the influence of diffusion on the dissolution of CO_2 in water over the long term. Molecular diffusion from the gas bubbles to the water causes a hydro-dynamically unstable layer, thus leading to the development of convective currents in the formation (Audigane et al., 2007). In this manner, diffusion results in more dissolved CO_2. In addition, the presence of diffusion increases the amount of free-phase CO_2 in the caprock but does not lead to more trapping by the caprock because of the reduction in the amount of dissolved CO_2 (Fig. 19).

6.2.2. *Reservoir Depth*

The depth of the storage and sequestration site is directly correlated with the hydrostatic pressure in the reservoir. Reducing the reservoir depth reduces the pressure. Some CO_2 properties, such as density, solubility and viscosity, change with pressure, and this pressure reduction reduces both solubility and density. A reduction in CO_2 density increases the buoyancy forces and results in an increase in the flow rate from the fracture outlet (Fig. 24). Furthermore, a reduction in CO_2 solubility reduces the amount of dissolved CO_2 and consequently increases the leakage rate.

6.2.3. *Groundwater Flow*

Groundwater flow is included in the simulation by adding constant hydrostatic pressure to the right boundary of the reservoir layer. The presence of pressure variations causes advection, and the CO_2 plume moves in the direction of flow or from higher pressure to lower pressure in the left boundary. The leakage of CO_2 in this scenario is higher than in the Base scenario during the first 100 years. However, after this time, flow rate decreases suddenly. The pressure increase in the reservoir due to groundwater flow is the reason for the increased leakage in the short term. Moreover, groundwater flow in the direction of the fracture causes the increased transport of CO_2, thereby increasing the leakage. However, after 100 years, the CO_2 at the bottom of the fracture is decreased to such an extent that the flow rate in the fracture becomes smaller than in the Base scenario (Fig. 31).

6.2.4. *Aquifer Liquid Flow*

Groundwater flow in the aquifer layer acts as a hydraulic barrier, and after 20 years, the CO_2 leakage stops (Fig. 31). Higher pressure in the aquifer layer creates a downward brine flow in the fracture and prevents the upward migration of CO_2 that is driven by buoyancy forces at the end of the injection period. The downward flow in the fracture changes the CO_2 plume in the reservoir (Fig. 32).

6.2.5. *Salinity*

Salinity leads to a residual trapping of CO_2 but also reduces the solubility of CO_2 in the formation fluid. In the short term, this residual trapping causes less CO_2 to leak into the aquifer layer in the brine compared with the base scenario, which is simulated for pure water (Fig. 35). However, as time passes, the solubility effect plays a more important role than residual trapping. After 25 years, the amount of CO_2 in the aquifer layer starts to increase in the saline aquifer. In fact, by reducing solubility, more free-phase CO_2 would leak into the aquifer because free-phase CO_2 has a lower density than water and moves upward due to buoyancy forces.

6.2.6. *Fracture Modeling Approach*

Fracture modeling approaches are not a feature of the system domain, but they have a strong influence on the simulation and modeling results of the CO_2 sequestration system. The results support this statement (Fig. 39). The choice of approach to use depends on observations, and borehole tests from the fracture zone may reveal a fracture zone at the site.

6.2.7. *Modifying Simulation*

In this study, a simple 2-D model was used for a hypothetical site. Using a 3-D model with more geometrical data for a real case study would provide a more precise simulation. In addition, using code TOUGH2 limits several processes and features in the simulation. The number of model elements is limited to several thousand, which is not sufficient to represent a large-scale situation with the necessary element sizes. An extension of the model domain might provide more accurate results in two ways. First, it could reduce the CO_2 flow from the left and right boundaries. Second, constant pressure in the boundary conditions in the model could provide less pressure to the injection elements. In addition, using reactive transport and flow could be useful to examine the combined influence of chemical reactions and transport processes on the

leakage rate. Finally, a sensitivity analysis for the various scenarios could be beneficial.

7. CONCLUSIONS

According to the simulation results, several conclusions can be drawn. First, including diffusion might provide more accurate results in the CO_2 sequestration system, but this is not necessary for a short-term simulation. Second, the reservoir depth, which led to pressure and density changes, also led to more leakage; on the other hand, it also provided a more stable plume in the reservoir layer. To continue, the groundwater flow could have both increasing and reducing effects on the leakage amounts. When there is groundwater flow in the reservoir layer, leakage increases; however, the rate of this leakage reduces over the long term. Groundwater flow in an aquifer would reduce the risk of CO_2 leakage. On the basis of only one simulation, it is difficult to say whether salinity would reduce or increase the leakage, as salinity may have different effects on the CO_2 flow rate. Fracture modeling approaches would provide different spatial results in the short term. Choosing an appropriate method depends on site observation.

REFERENCES

Audigane P, Gaus I, Czernichowski LI, Pruess K, Xu T. 2007.Two-dimensional reactive transport modeling of CO2 injection in a saline aquifer at the sleipner site, North Sea.American Journal of Science. 307:974–1008.

Bachu S, Gunter WD, Perkins EH. 1994. Aquifer disposal of CO2: Hydrodynamic and mineral trapping. Energy Conversion and Management. 35:269–279.

Bachu S. 2000. Sequestration of CO2 in geological media: Criteria and approach for site selection in response to climate change. Energy Conversion and Management. 41: 953–970.

Bachu S. 2003. Screening and ranking of sedimentary basins for sequestration of CO2 in geological media in response to climate change. Environmental Geology. 44:277-289.

Bachu S. 2008. CO2 storage in geological media: role, means, status and barriers to deployment. Progress in Energy and Combustion Science. 34:254–273.

Bielinski, A. 2006.Numerical simulation of CO2 sequestration in geological formations.PhD.Universität Stuttgart.

Bouc O, Audigane P, Bellenfant G, Fabriol H, Gastine M, Rohmer J, Seyedi D. 2009. Determining safety criteria for CO2 geological storage.*EnergyProcedia*. 1:2439-2446.

Bowden AR, Rigg AJ. 2004. Assessing risk in CO2 storage projects. Australian Petroleum Production Exploration Association Journal. 44:677–702.

Celia MA, Nordbotton JM. 2009. Practical modelling approaches for geological storage of carbon dioxide. Ground Water, 47:627–638.

Cooper C. 2009. A technical basis for carbon dioxide storage.EnergyProcedia. 1:1727-1733.

Damen K, Faaij A, Turkenburg W. 2006. Health, safety and environmental risks of underground CO2 storage—overview of mechanisms and current knowledge.Climate Change. 74:289–318.

Gasda SE, Bachu S, Celia MA. 2004. Spatial characterization of the location of potentially leaky wells penetrating a deep saline aquifer in a mature sedimentary basin. Environmental Geology. 46:707-720.

Gaus I. 2010.Role and impact of CO2-rock interaction during CO2 storage in sedimentary rocks.International Journal of Greenhouse Gas Control. 4:73-89.

Hassanzadeh H, Pooladi-Darvish M, Keith DW. 2009. Accelerating CO2 Dissolution in Saline Aquifers for Geological Storage–Mechanistic and Sensitivity Studies. Energy and Fuels. 23:3328–3336.

Hesse MA. 2008. Mathematical modeling and multiscale simulation for CO2 storage in saline aquifers. PhD Stanford University, USA.

Holloway SH, Savage D. 1993. The potential for aquifer disposal of carbon dioxide in the UK.Energy Conversion Management. 34:925–932.

Kreft E, Bernstone C, Meyer R, May F, Arts R, Obdam A, Svensson R, Eriksson S, Durst P, Gaus I, van der Meer B, Geel C. 2007. The Schweinrich structure, a potential site for industrial scale CO2 storage and a test case for safety assessment in Germany. International Journal of Greenhouse Gas Control.1:69–74.

Kumar A, Ozah R, Noh M, Pope GA, Bryant S, Sepehrnoori K, Lake LW. 2005. Reservoir simulation of CO2 storage in deep saline aquifers. Society of Petroleum Engineers Journal. 10:336-348.

Leonenko Y, Keith DW. 2008. Reservoir engineering to accelerate the dissolution of C02 stored in aquifers. Environmental Science & Technology 42:2742-2747.

Li Z, Dong M, Li S, Huang S. 2006.CO2 sequestration in depleted oil and gas reservoirs—caprock characterization and storage capacity.Energy Conversion and Management. 47: 1372–1382.

Maul PR, Savage D, Benbow SJ, Walke RC, Bruin R. 2005. Development of a FEP Database for the Geological Storage of Carbon Dioxide. Proceedings of the Seventh International Conference on Greenhouse Gas Control Technologies, Vancouver, Canada, 1:701-710.

Narasimhan TN, Witherspoon PA. 1976. An Integrated Finite Difference Method for Analyzing Fluid Flow in Porous Media. *Water Resources Research*. 12:57–64.

[i]Oldenburg CM. 2008. Screening and ranking framework for geologic CO2 storage site selection on the basis of health, safety, and environmental risk. Environmental Geology. 54:1687–1694.

Oldenburg CM, Bryant SL, Nicot JP. 2009. Certification framework based on effective trapping for geologic carbon sequestration. International Journal of Greenhouse Gas Control. 3:444–457.

Pruess K, 1991.Tough2 A General Purpose Numerical Simulator for Multiphase Fluid and Heat Flow,.LBNL-29400. Lawrence Berkeley Natl. Lab., Berkeley, CA. 102p.

Pruess K, Oldenburg CM, Moridis G. 1999.Tough2 User's guide, Version 2.0.LBNL-43134. Lawrence Berkeley Natl. Lab., Berkeley, CA. 198p.

Pruess, K., Spycher, N. 2007. ECO2N – A fluid property module for the TOUGH2 code for studies of CO2 storage in saline aquifers. Energy Conservation and Management, 48:1761-1767.

Riddiford FA, Tourqui A, Bishop CD, Taylor B, Smith M. 2003. A cleaner development: the In Salah gas project, Algeria. In: *Proceedings of the 6th international conference on greenhouse gas control technologies vol. I*, Gale JJ, Kaya Y. (Eds).Pergamon:Amsterdam. 601–606.

Rish WR. 2005. A probabilistic risk assessment of Class I hazardous waste injection sites. In: *Underground Injection Science and Technology*, *Developments in Water Science*, Tsang CF, Apps JA. (Eds) 52:93–125.

Savage D, Maul PR, Benbow S, Walke RC. 2004. A generic FEP database for the assessment of long-term performance and safety of the geological storage of CO2. *Quintessa Report* QRS-1060A-1

Sminchak J, Gupta N, Byrer C, Bergman P. 2002. Issues related to seismic activities induced by the injection of CO2 in deep saline aquifers. Journal of Energy and Environmental Research. 2:32–46.

Solomon S, Carpenter M, Flach TA. 2008. Intermediate storage of carbon dioxide in geological formations: a technical perspective. International Journal of Greenhouse Gas Control. 2: 502–510.

Span R, Wagner W. 1996. A New Equation of State for Carbon Dioxide Covering the Fluid Region from the Triple–Point Temperature to 1100 K at Pressures up to 800 MPa. Journal of Physical and Chemical Reference Data. 25:1509–1596.

Stauffer PH, Viswanathan HS, Pawar RJ, Guthrie GD. 2009.A system model for geologic sequestration of carbon dioxide, Environmental Science and Technology. 43:565–570.

Swift P, Barr G, Barnard R, Rechard R. 1999. Feature, Event, and Process Screening and Scenario Development for: The Yucca Mountain Total System Performance Assessment. In *Scenario development methods and practice: an evaluation based on the NEA Workshop on Scenario Development.*OECD Nuclear Energy Agency (Ed). OECD: Madrid. 240p.

Van der Zwaan B, Smekens K. 2009. CO2 capture and storage with leakage in an energy-climate model.Environmental Modeling Assessment. 14:135–148.

Van Egmond B. 2006. Developing a method to screen and rank geological CO2 storage sites on the risk of leakage. Copernicus Institute. Department of science, technology and society.NWS-E-2006-108.

Wu Y-S, Qin G. 2009. A generalized numerical approach for modeling mulitphase flow and transport in fractured porous media, Communications in Computational Physics. 6:85–108.

Xu T, Apps JA, Pruess K. 2004. Numerical simulation of CO2 disposal by mineral trapping in deep aquifers.Applied Geochemistry. 19:917–936.

Yang F, Bai BJ, Tang DZ, Dunn-Norman S, Wronkiewicz D. 2010.Characteristics of CO2 sequestration in saline aquifers.Petroleum Science. 7:83–92.

Zheng L, Apps JA, Zhang Y, Xu T, Birkholzer JT. 2009. On mobilization of lead and arsenic in groundwater in response to CO2 leakage from deep geological storage.Chemical Geology. 268:281–297.

APPENDIX I – EXTRA EQUATION IN TOUGH2

More explanations regarding these equations can be found in the Tough2's User's guide (Pruess et al., 1999).

Description	Equation
Pressure and capillary pressure	$P_\beta = P + P_{c\beta}$
Henry's law	$P_g^K = K_H x_{aq}^K$
Relative Permeability	$if\ S_l < S_{ls}, \quad k_{rl} = \sqrt{S^*}\ \left\{1-\left(1-\left[S^*\right]^{1/\lambda}\right)^{\lambda}\right\}^2$ $if\ S_l \geq S_{ls}, \quad k_{rl} = 1$ $if\ S_{gr} = 0 \quad k_{rg} = 1 - k_{rl}$ $f\ S_{gr} \geq 0 \quad k_{rg} = (1-\hat{S})^2(1-\hat{S}^2)$ $where \quad S^* = (S_l - S_{lr})/(S_{ls} - S_{lr}),$ $\hat{S} = (S_l - S_{lr})/(1 - S_{ls} - S_{lr})$
Capillary pressure	$P_c = P_0([S^*]^{-1/\lambda} - 1)^{1-\lambda}$ $subject\ to \quad P_{\max} \leq P_c \leq 0$
Molecular diffusion	$f_\beta^{\mathrm{K}} = -\Phi \tau_0 \tau_\beta \rho_\beta d_\beta^{\mathrm{K}} \nabla X_\beta^{\mathrm{K}}$ $where \quad \tau_0 \tau_\beta = \tau_0 k_{r\beta}^{(S_\beta)}$ $d_\beta^{\mathrm{K}}(P,T) = d_\beta^{\mathrm{K}}(P_0,T_0)\frac{P_0}{P}\left[\frac{T+273.15}{273.15}\right]^\theta$

These symbols are explained below.

Symbol descriptions

Greek Symbol	
β	Phase index [subscript]
θ	Exponent for the temperature dependence of diffusivity
K	Mass Component [superscript]
λ	Van Genuchten's[m]
Φ	Porosity
τ	Tortuosity
ρ	Density [kg/m^3]
Subscripts and Superscript	
g	Gas
l	Liquid
max	maximum
r	Residual
w	Water
0	Reference Value
List of Symbols	
P_c	Capillary Pressure [pa]
P	Total pressure [pa]
d	Molecular diffusivity
k_r	Relative Permeability
S	Saturation
T	Temperature

APPENDIX II. INITIAL AND BOUNDARY VALUES FOR ALTERNATE SCENARIOS

Initial and boundary conditions for the Alternate Scenarios

Scenario A-1:No fracture zone is present in the caprock

Initial conditions and boundary values are as same as in the Base scenario, and the only change is in considering that the fracture zone has the same permeability as the caprock layer

Scenario A-2:Diffusion is not considered as a transport process

Setup in simulation

Scenario A-3:System depth is changed and is located at a depth of 600 m below the ground surface

Boundary	Type	Variable	Value	Unit	Comment
Left & Right	Dirichlet	P	60.0E5+ 9.80*z(m)	Pa	The only difference from the Base scenario

Scenario A-4: Flow of water in reservoir layer

Boundary	Type	Variable	Value	Unit	Comment
Left & Right	Dirichlet	P	60.0E5+ 9.80*z(m)	Pa	The only difference from the Base scenario

Scenario A-5:Flow of water in aquifer layer

Boundary	Type	Variable	Value	Unit	Comment
Left & Right	Dirichlet	P	60.0E5+ 9.80*z(m)	Pa	The only difference from the Base scenario

Scenario A-6:Formation fluid has a salinity of 10 ppm

Variable	Value	Unit	Comment
Salt mass fraction (Xcm)	0.00	ppm	

Scenario A-7:Using ECM instead of DCM

Scenario A-8:Using MINC instead of DCM

APPENDIX III. ADDITIONAL RESULTS

Scenario A-2 (Only Advection)

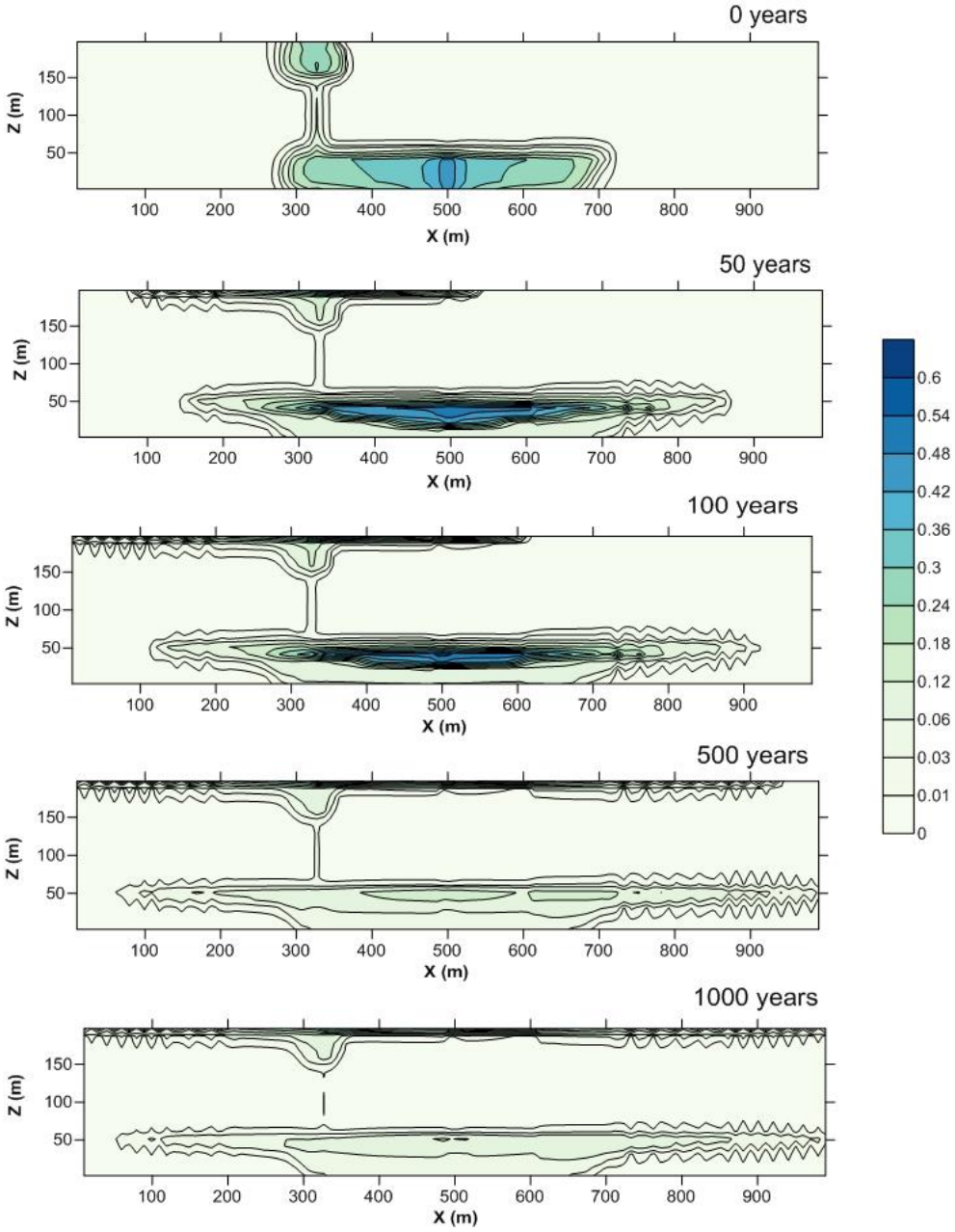

Supercritical CO_2 gas phase (SG) migration in the system without diffusion (Scenario A-2) simulated from the end of the injection period until 1,000 years later.

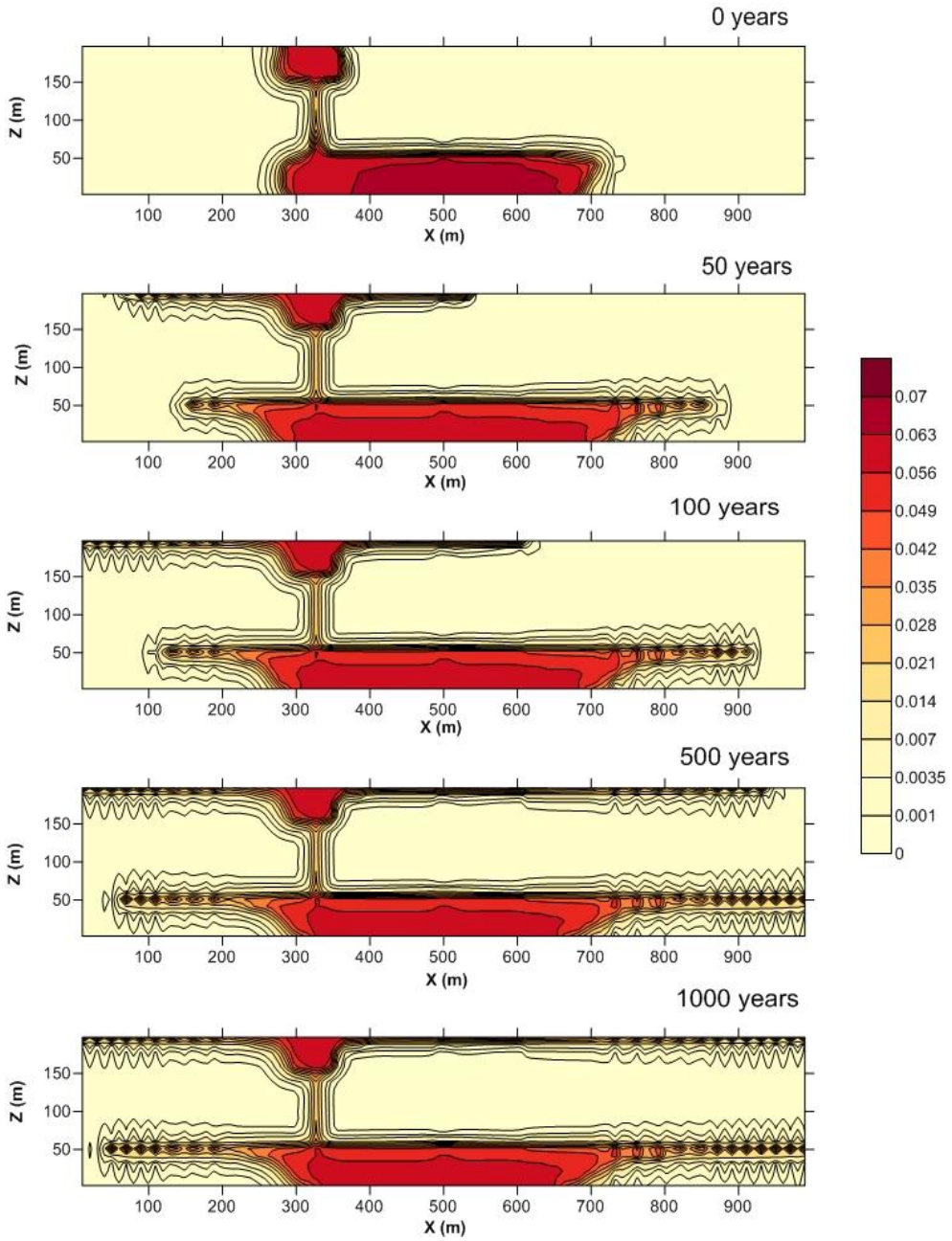

Mass fraction of CO2 in the water (XCO2L) for only advection (scenario A-2) simulated from the end of the injection until 1,000 years later.

Scenario A-7 (Equivalent porosity method)

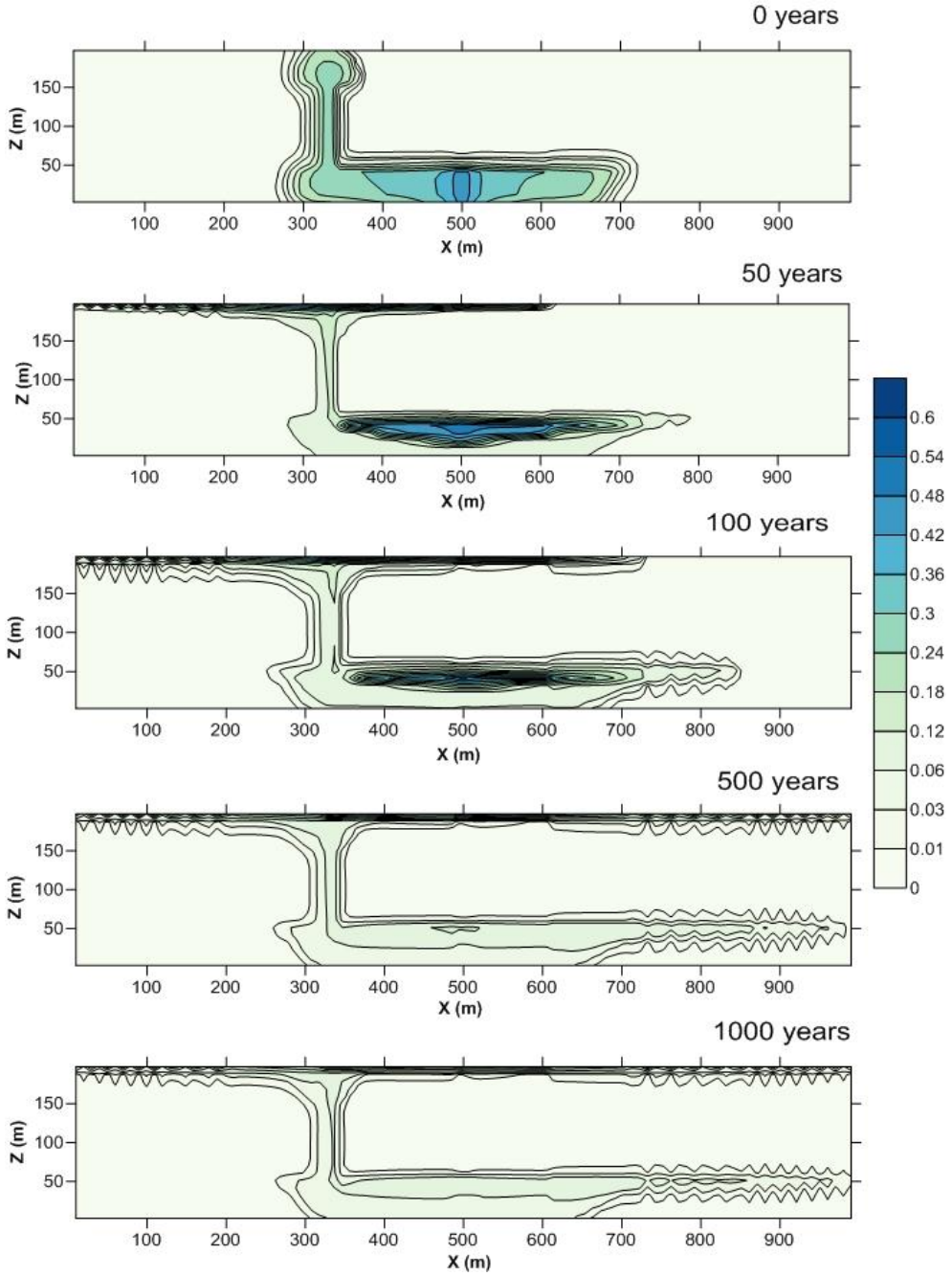

Supercritical CO_2 gas phase (SG) migration in the system with Scenario A-7 simulated from the end of the injection period until 1,000 years later.

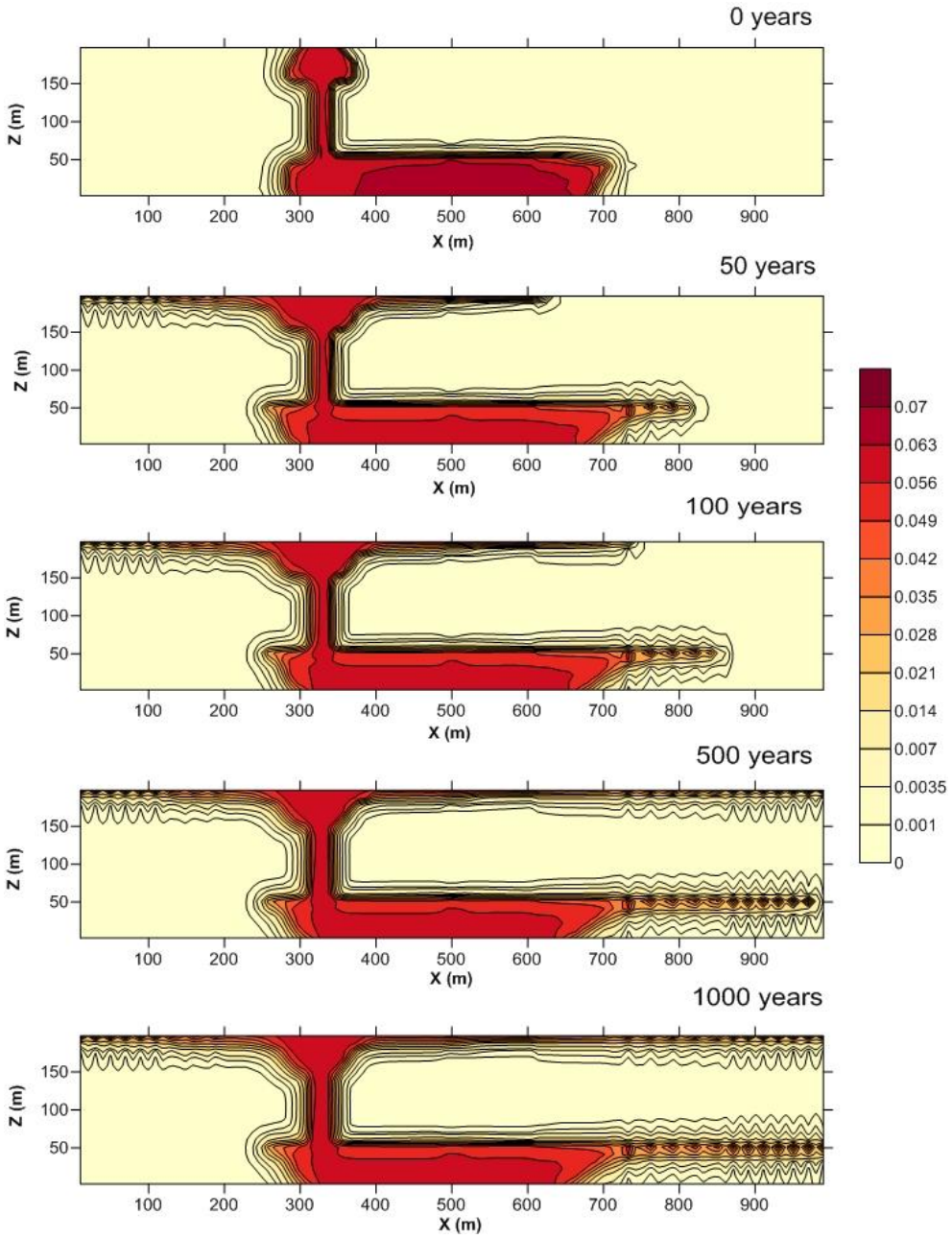

Mass fraction of CO2 in the water (XCO2L) (Scenario A-7) simulated from the end of the injection period until 1,000 years later.

Scenario A-8 (Multi porosity method)

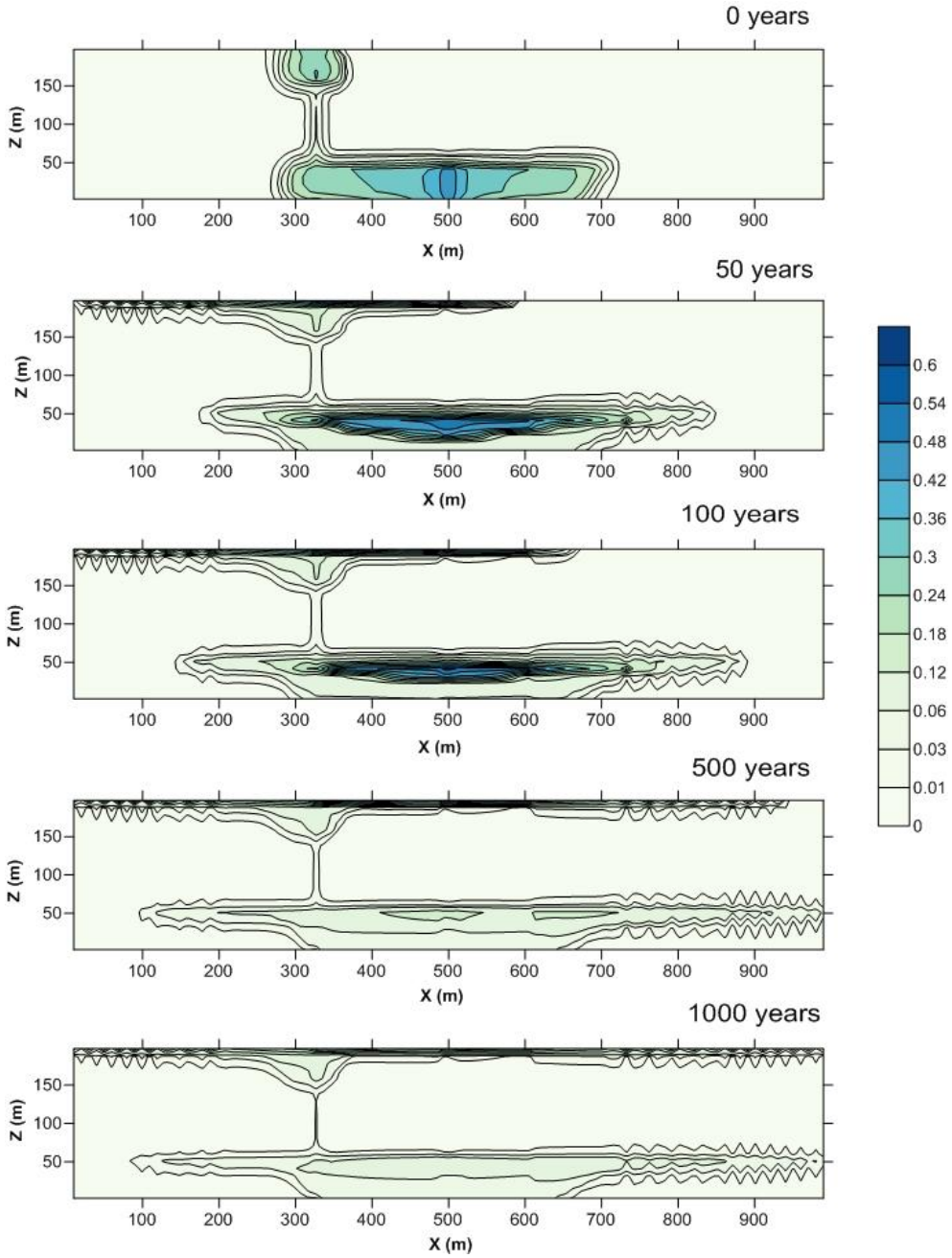

Supercritical CO_2 gas phase (SG) migration in the system with Scenario A-8 simulated from the end of the injection period until 1,000 years later.

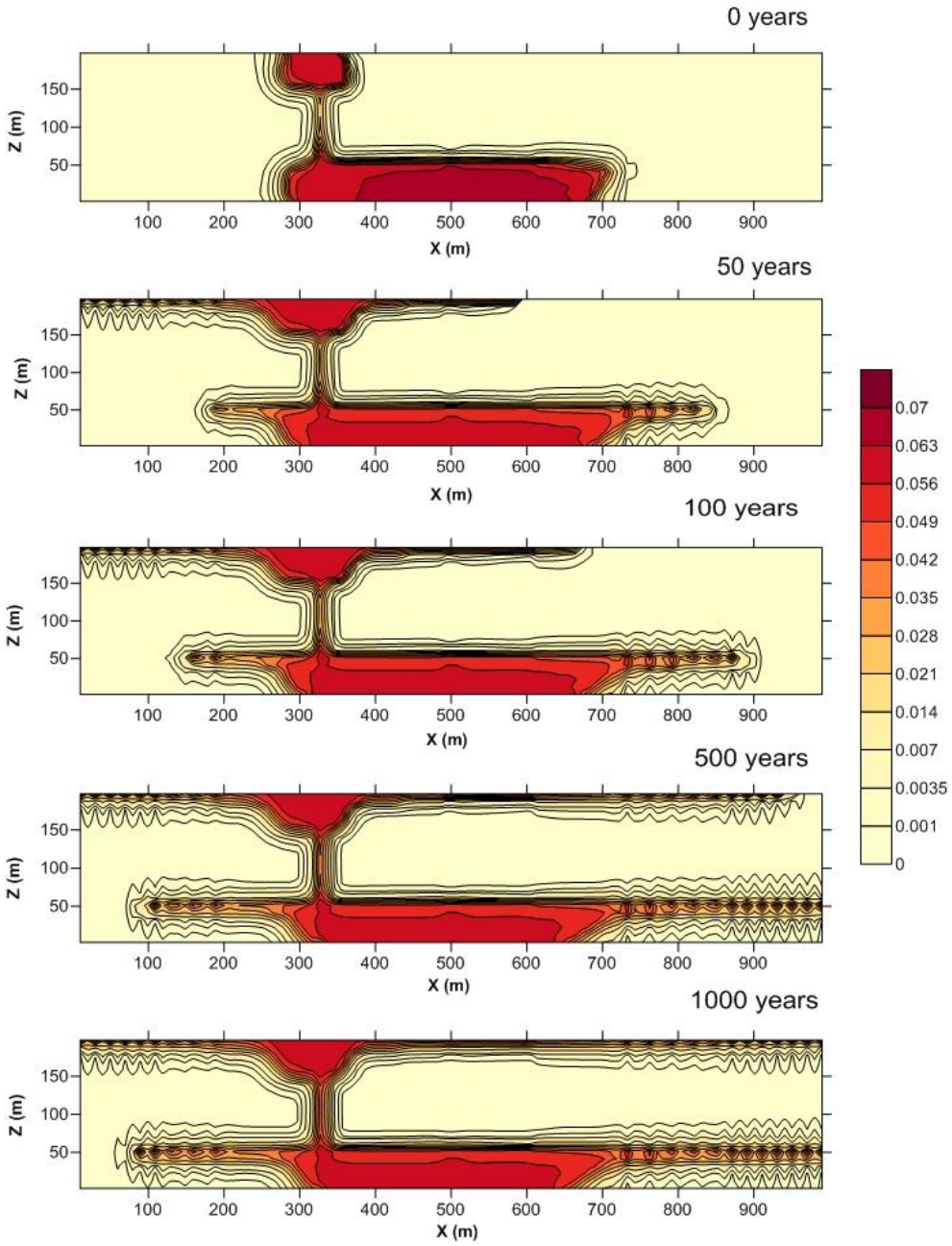

Mass fraction of CO_2 in the water (XCO2L) (Scenario A-8) simulated from the end of the injection period until 1,000 years later.